Seismic Zoning and Seismic Ground Motion in the Southern Parts of Kyoto, Southwest Japan

By Junpei AKAMATSU

(Manuscript received December 11, 1985)

Abstract

The vibrational characteristics and the process of vibration during earthquakes were examined in regard to the source properties, seismic wave attenuations and amplification effects of soil grounds.

In and around the Kinki district, Southwest Japan, the regional variations of stress drop and attenuation, depending on the geological structure and the regional seismic activity, have been obtained from coda analysis for small earthquakes of $M<5$. The effects of source properties were investigated for larger events with magnitude of up to 6.8 by the time domain analysis and the response spectral analysis. It was found that the high frequency vibrational characteristics reflect the regionality of stress drop derived from small events. As a result, large acceleration even by moderate earthquake may be predicted in the northernmost region of the Kinki district, where high stress drop and small attenuation have been suggested.

The long period seismic effects due to the soil deposits in the Kyoto basin have been studied by observation of microseism caused mainly by sea waves. The process of vibration during the 1984 West Nagano Prefecture Earthquake was examined in relation to the ground characteristic frequency inferred from microseism. The amplification by soil deposits was explained with the amplification and elongation of duration for each wave mode and the resultant interference of various modes in the characteristic frequency. It was suggested that the amplification factor for microseism corresponds to the maximum value of that for seismic surface waves.

The instrumentation and the method of seismometry at the Sumiyama Seismic Observatory of Kyoto University will be described briefly.

In the Appendix, the regional variations of attenuation for seismic coda, Q_c^{-1}, observed in and around the Kinki district are mentioned.

Contents

1.	Introduction	2
2.	The Sumiyama Seismic Observatory (**SUM**) and surrounding geological structure and seismicity	3
3.	Observational systems at **SUM**	4
3.1	The symmetrical three-component seismograph system (**SYM**)	6
3.2	The digital strong motion seismograph system (**SMS**)	7
3.3	Listing of data files in the analog magentic tape	9
4.	Attenuation of seismic wave	11
5.	Regional variation of source property and its effects on vibrational characteristics	13
5.1	M_0-f_c relation inferred from coda analysis	14
5.2	Variation of vibrational characteristics with source location	16
6.	Vibrational characteristics of soil ground in the Kyoto basin	20
6.1	Seismic amplification due to soil deposits inferred from microseism	22
6.2	Amplification of crustal surface waves from near earthquakes	23
6.3	Long period vibrational characteristics during the 1984 West Nagano Prefecture Earthquake	23

7. Discussion 28
8. Conclusion 30
References 31
Appendix 1. Equation of motion for inclined seismometer and calibration method 34
Appendix 2. Regional variation of Q_c^{-1} 36

1. Introduction

In the study for elucidation and prediction of seismic ground motion, the problems are usually discussed with three factors: source, path and site. As for the source property, the regional variation of source spectra was observed in and around the Kinki district, Southwest Japan[1,2]. Hirano examined the S wave spectra for moderate and small earthquakes and discussed the regional variation of tectonic stress in relation to the seismic activity and aftershock activity in the vicinity of Kyoto, in the Kinki district[1]. Furuzawa et al. showed that the predominant frequencies of body waves from micro earthquakes varied with source location depending on the seismic activity in the southern parts of Kyoto[2]. In our previous study the regional variation of stress drop was examined with coda analysis for small events in and around the Kinki district[3]. This regional variation is very interesting for study of seismic ground motion, because the stress drop may closely relate to high frequency excitation of S_g and L_g waves.

In this paper we summarize the previous results: the seismic wave attenuation and source spectra derived from coda analysis for the small events of $M<5$. And we examine the wave form and the response spectra of larger events observed with the digital strong motion seismograph system (**SMS**) at the Sumiyama Seismic Observatory (**SUM**) to find the effects of the source properties suggested from the coda analysis of small events.

As for the path effects, we discussed seismic wave attenuations with various analyzing procedures to obtain the frequency dependent Q_s^{-1}[3]. The regional variation of coda decay was observed in the area in relation to the geological structure. From this we discuss the applicable range and region for the S wave attenuation, Q_s^{-1}.

As for the site property, it is one of the important problems how the excitation of the long period components above 1 sec in a strong motion seismogram at a soil ground is related to the deep geological structures[4]. Many efforts have been made to evaluate the seismic effects due to such deep structures as the depth of bed rock is over 100 m[e.g.5]. In this respect, the vibrational characteristics of microseism were examined in the Kyoto basin[6], and the amplifications of surface waves due to the soil deposits were evaluated in the previous work[7]. These results were based on the spectral features, therefore, the details of the process of vibration by various wave modes during earthquake have not been clarified. As the duration is an important factor in the vibrational characteristics of long periods (as in the problem of oil-slosh in a large tank), the process of vibration must be examined. The 1984

West Nagano Prefecture Earthquake (M 6.8) was well recorded by **SMS** at **SUM** and the Seismic Station in the Uji Campus of Kyoto University. The seismograms were characterized with strong excitation of the long period crustal surface waves following high frequency S_g waves[8].

In this paper, we examine the effects of soil ground on various wave modes and the process of vibration during the earthquake by use of the band-pass-filters and response spectral analysis, from which we discuss the meaning of the amplification factors inferred from microseism.

Our discussion is based on the observational data mainly at **SUM**, where the two seismograph systems were designed and set up for the accurate and reliable seismometry, that is, the symmetrical three-component seismograph system with analog magnetic recording (**SYM**)[9] and the digital strong motion seismograph system utilizing the magnetic bubble memory (**SMS**)[10]. We describe the systems and the method of seismometry at **SUM**.

2. The Sumiyama Seismic Observatory (SUM) and surrounding geological structure and seismicity

The **SUM** was set up in March 1976 on an outcrop of the Paleozoic strata with an usual three-component seismograph. From July 1976 the magnetic seismograms in analog form have been obtained routinely. The seismometers were changed to the symmetrical three-component ones in December 1979. The digital strong motion seismometry started in July 1981.

Around **SUM**, the wave velocities of the surface layer, which is considered as the Paleozoic complex, were estimated to the depth over 750 m as V_p=4.66 km/sec and V_s=2.58 km/sec[11].

As the directivity and linearity of vibration are the most basic data for study of wave field, the site property was examined with particle motion analysis, from which it was ascertained that the seismogram was fit to the wave form analysis up to the frequency range above 25 Hz[12].

Fig. 1 shows the geological structure in and around the Kinki district, Southwest Japan[13,14]. Southwest Japan can be divided into the Inner Zone and the Outer Zone by a major fault, the Median Tectonic Line (**MTL**). The tectonic divisions parallel to the general trend of the island arc are distinct, although not so clear in the Inner Zone as the Outer Zone. The Shimanto belt in the Outer Zone is known to be the youngest in the tectonic divisions.

Figs. 2 and **3** are referred to see the seismic activity in the area[15]. It is well known that the Outer Zone is tectonically more active than the Inner Zone as seen from **Fig. 2**(**B**), which shows the seismicity of the depth of 30–80 km. Small and micro earthquakes occur frequently, often in a swarm, near Wakayama in the Outer Zone as shown in **Fig. 2**(**A**). In the Inner Zone seismic activity is high in the zone from the Lake Biwa to the Osaka bay, while it is very low in the south and east

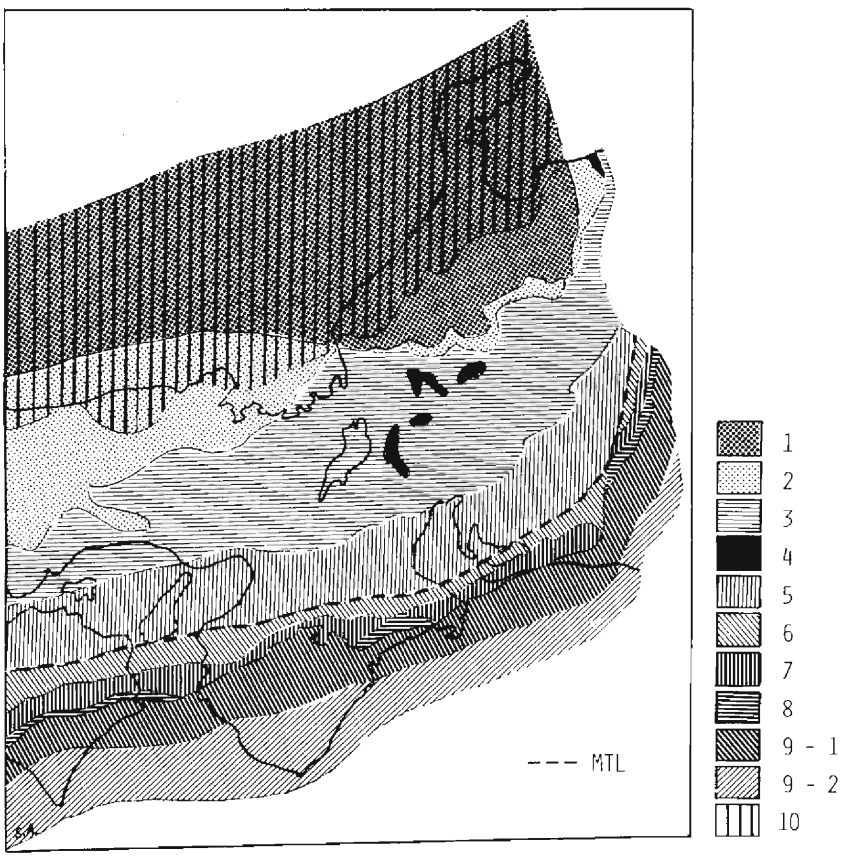

Fig. 1 Gross geological structure in and around the Kinki district. 1: Hida zone, 2: Sangun zone including Hida tectonic zone and Maizuru zone, 3: Tanba and Mino zone, 4: Paleozoic strata of Akiyoshi phacies, 5: Ryoke zone, 6: Sanbagawa zone, 7: Chichibu zone, 8: Sambosan group, 9–1: North Shimanto belt, 9–2: South Shimanto belt, 10: Green taff region. Arranged from the Map of the geological structure in Atlas Japan, Geological Survey, Japan[14].

region to the zone, that is, Nara and Mie prefectures. The **SUM** is located nearly on the boundary of these regions.

3. Observational systems at SUM

In the first stage of data processing for seismograms, it is necessary to identify the wave type. Two kinds of direction, that is, propagational direction of wave and vibrational direction of ground, are the most basic information about the wave field. From this reason, a three-component seismograph is indispensable.

Recently the analysis has usually been carried out by computer, therefore, the seismogram must be in digital or digitizable form[16]. Magnetic recording system

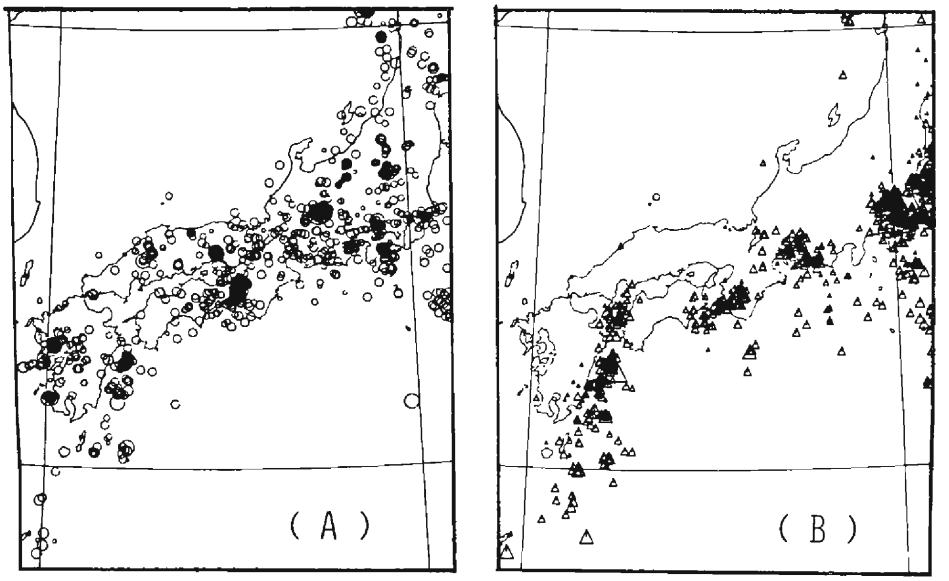

Fig. 2 Earthquake distribution in and near Japan, 1984. (A): H<30 km, (B): 30 km≦H<80 km. Reproduced from the Seismological Bulletin of JMA for Dec. 1984.

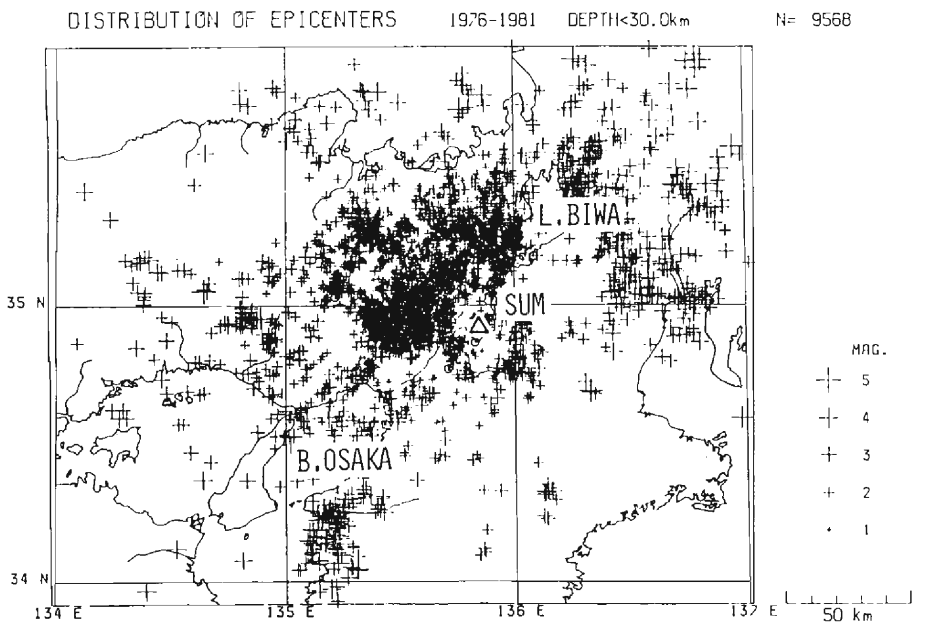

Fig. 3 Distribution of epicenters of microearthquakes with shallow foci (H≦30 km) observed by the telemetry network system for microearthquake obseravtion at Regional Center for Earthquake Prediction, Faculty of Science, Kyoto University, from 1976 to 1981. Reproduced from the paper by N. Maeda, and H. Watanabe (1984)[15].

operates in many stations in analog and/or digital form. However, in a strong motion observation, there remain some technical but inevitable problems in tape driving mechanism.

At **SUM**, two seismograph systems are operating for different observational objects, that is, the symmetrical three-component seismograph system with analog tape recorder for short period weak motion and the digital strong motion seismograph system utilizing magnetic bubble memory.

At **SUM** the "seismometry" includes the following functions: file listing of the analog magnetic tape, visualization of magnetic record, filing of the strong motion digital data on MT and calculation of their spectra. These functions run semi-automatically on a micro computer system, which is also used for the preliminary analyses such as Fourier analysis, particle motion analysis, filtering operation, and so on.

3.1 The symmetrical three-component seismograph system (SYM)[9]

In the three-component seismometry it is essential that the frequency response of each component is identical, and that the normal operation is able to be confirmed. In this regard it has been pointed out that the symmetrical system is superior to the usual system with a vertical and two horizontal components[17]. The symmetrical system is composed of three inclined seismometers, the sensitive direction of which makes an angle of 35°18′ to the horizontal plane (see **Appendix 1**), and which are

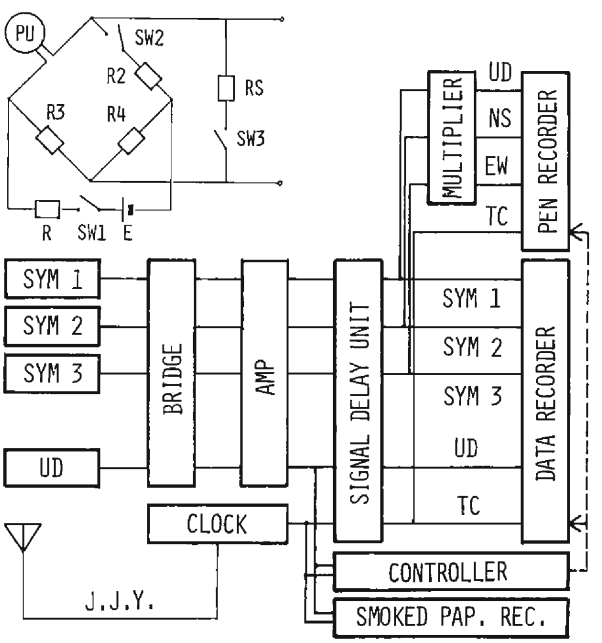

Fig. 4 Block diagram of the symmetrical three-component seismograph system.

set symmetrically with respect to the vertical line at interval of 120°. The total system responses are checked by observing tremors, when all seismometers are set in one direction.

Fig. 4 shows the block diagram of **SYM**. The symmetrical three components and the additional vertical component are recorded on the magnetic tape. In the analysis the vertical component is synthesized with the symmetrical three components and is compared to the original vertical one in confirmation of normal operation of all components[17]. This is particularly useful in observation of lower frequency components below the seismometer's natural frequency, 1 Hz. The pen-recorder serves the visible monitor seismogram, the components of which are synthesized into usual components (UD NS EW) for convenience of preliminary polarization analysis. One track on magnetic tape is used for identification information such as event number, triggering time, tape count, recording condition, and so on, which are used in the work of the file listing. **Photo 1** shows the symmetrical seismometer.

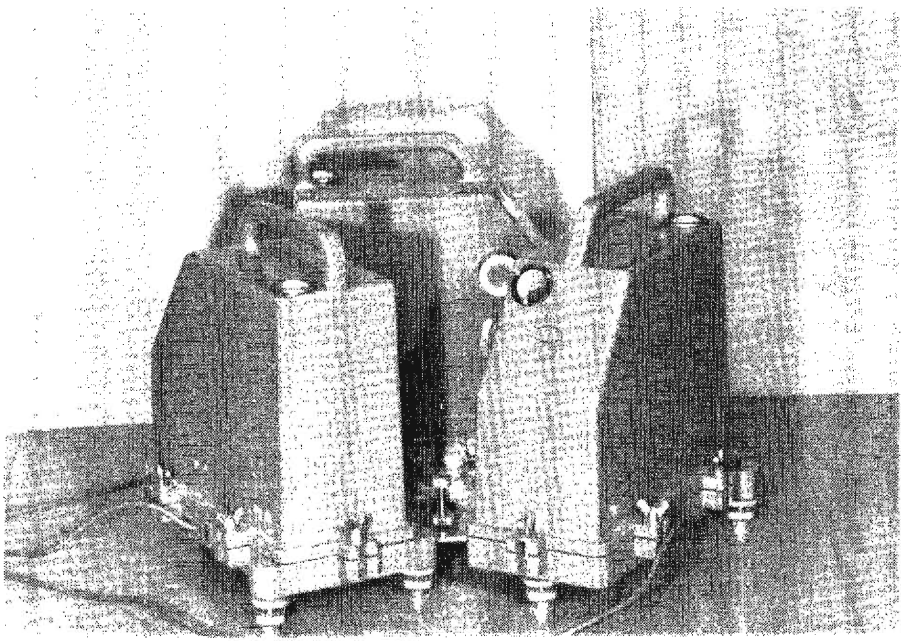

Photo. 1 The symmetrical three-component seismometer.

3.2 The digital strong motion seismograph system (SMS)[10]

In addition to the common performance of usual magnetic seismograph the basic conditions for strong motion seismograph are as follows: (1) long term reliability of system and recording medium with easy maintenance, (2) anti-shock performance, (3) perfect backup system for power failure. From the conditions of (1) and (2), there are some problems in a method of magnetic tape recording. In this regard, **SMS** was designed with two different recording media: the magnetic bubble

memory (**MBM**) for reliable data acquisition and storage during strong motion, and the cassette magnetic tape (**CMT**) for data transport. **MBM** is non-volatile, solid state memory and is shock-proof against acceleration exceeding 50 g. After the strong motion or the relief of earthquake damage, the data in **MBM** are transmitted to **CMT** automatically or manually.

Various transducers have been deviced for strong motion observation. However, the base for seismometers is apart from recording room by 400 m, therefore, the moving coil type electro-magnetic seismometers (f_0=3.0 Hz, h=12) are used. It is of great advantage to routine observation that the normal operation can be checked with calibration signal from the recording room. In order to widen the recording dynamic range, the acceleration signals are integrated with low pass filters to velocity seismograms.

Fig. 5 shows the block diagram of **SMS**. Earthquake motion is detected by monitoring the amplitude of vertical component (TRG 1). The sampling rate of A/DC is originally 100 Hz, however, is reduced to 50 Hz to prevent excessive amount of data for low frequency events, under the control of the comparator which monitors the high frequency components (TRG 2).

The micro-processor, Z-80, implements the signal processing algorithms, such as event triggering, selection of sample rate, digital low pass filtering operation for anti-aliasing of 50 Hz data, 12 bits to 10 bits data compression for economy of memory area, **CMT** control process with **CMT**'s failure diagonostic, and so on. **SMS** is supported with battery in the case of A.C. powre failure.

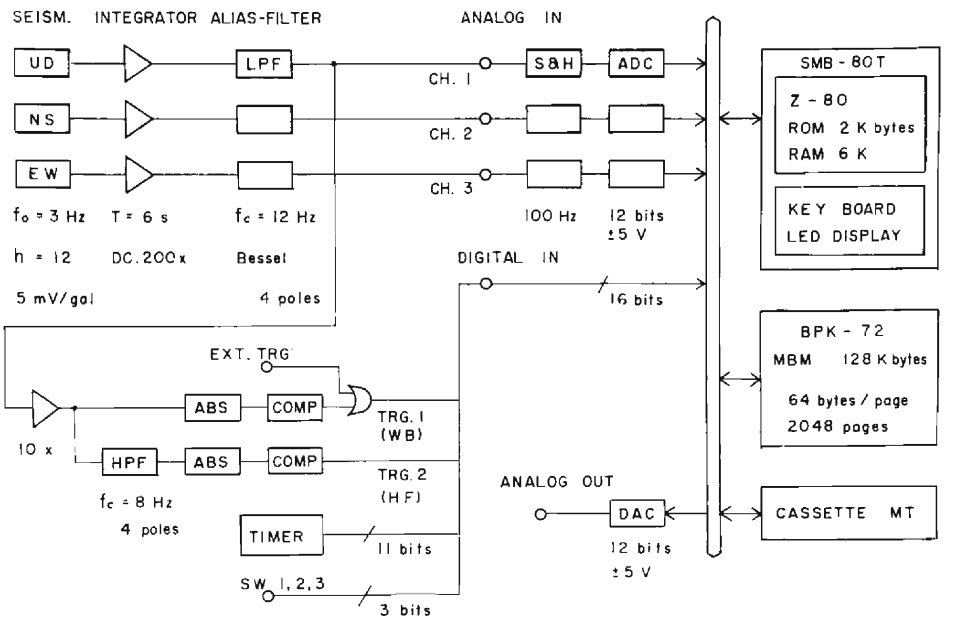

Fig. 5 Block diagram of the digital strong motion seismograph system.

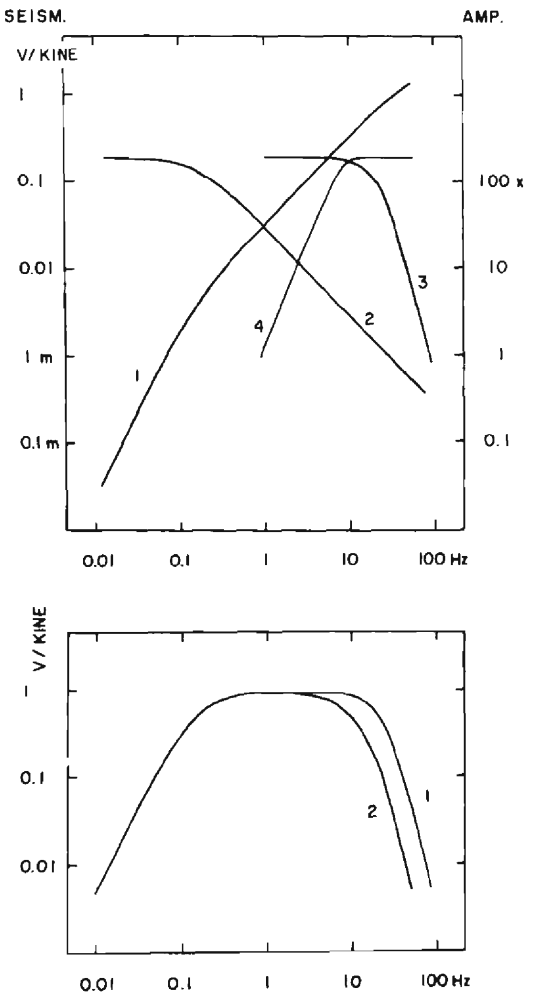

Fig. 6 Frequency characteristics of the elements of the SMS and system response. Upper: 1–seismometer (5 mV/gal, $h=12$) figured in velocity scale, 2–preamplifier with integral characteristics ($\tau=6.28$ sec), 3–anti alias filter, 4–high pass filter for trigger and sample rate logic. Lower: overall responses in velocity scale, 1–100 Hz sampling, 2–50 Hz sampling with digital low pass operation.

At **SUM**, **SMS** operated without any troulbe from July 1981 and has recorded the ground motion over about 0.03 kine. **Fig. 6** shows the frequency responses. **Table 1** lists the specifications of the system.

3.3 Listing of data files in the analog magnetic tape

Furuzawa critically discussed some problems on the methods of digital data acquisitions[16]. In the case of digital recording, an observational system is usually

Table 1 Specification of the **SMS** system

Analog In	3ch. ADC: 12 bits, sample rate: 100 Hz (50 Hz) dynamic recording range 66 db, (max. ±5.5 kine) resolution 54 db, (2.7 m kine/dig)
Digital In	16 bits (TRG. 1, TRG. 2, Time Code 11 bits, SW 1, 2, 3)
Analog Out	1ch. DAC: 12 bits, ±5 v
Delay Time	14.08 sec
Recording Time	MBM: 5 m 27 s (100 Hz), 10 m 54 s (50 Hz) CMT: 9 m 30 s (100 Hz), 19 m (50 Hz)

supported by a mini- or micro-computer. Therefore, the listing of the events with various observational information is rather easy either in on-line mode or in off-line mode[18]. In the case of analog magnetic recording, however, the event detection and system controls are implemented by a hard logic circuit, and the full listing may not be rendered at the observational time. Therefore, the listing of events in the analog magnetic tape recorded is an important work to be carried out first.

At **SUM** this work is carried out semi-automatically with a micro-computer system, the set-up of which is shown in **Fig. 7.** In our seismometry the automated listing is one of the most useful programs.

First, the system reads the identification information on the analog magnetic tape through GPIB (general purpose interface board) and files them on a floppy disk. And then the system analyzes the events to get maximum amplitudes and duration times in which the amplitudes exceed a given threshold level with use of A/DC. The procedures run automatically. In seismometry it is one of the basic operations to group the events. In the present state we group the events manually into several types according to S–P time and cause of events (natural earthquake or quarry blast...)[12]. Finaly the information on the floppy disk is refiled on MT with the event type. The MT files are used for selecting and listing the events under given conditions such as event type, amplitude level and duration time. **Fig. 8**

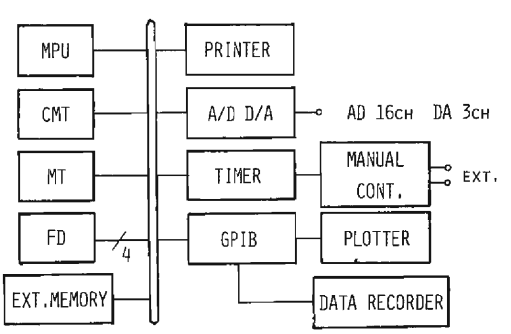

Fig. 7 Set-up of micro-computer system for seismometry at **SUM.**

```
XR-310 EVENTS SELECTED WITH THE FOLLOWING CONDITIONS

    SELECTING GROUPS  L  M  N
    EXCLUDING GROUPS  X  T  Q
    EXCLUDING THE EVENT WITH IMPERFECT INITIAL MOTION
    EXCLUDING THE EVENT WITH ERROR COMPONENTS
                    THRESHOLD LEVEL (M V)   100   100   100   100   ( AT LEAST ONE CH OVERS )

    SUM- 37    *** AMP=SA-16 50* (CH.4 L4*100)  DELAY=SD-12  AZM=N X E

               *** TS=8    RANGE=05.05.05.05.06.05.05    SERVO=101 ***

NO  IDNO  COUNT   Y  M  D   H  M                    CH.  1    2    3    4   G   INT   ERR.CH

 1  1244  030.6  85 07 25  05 48  MAX AMP  (M V)   119  190  192  112  N
                                  DURATION (SEC)     1    2    2    0

 2  1245  033.4  85 07 25  09 00  MAX AMP  (M V)   163   85  104   85  M
                                  DURATION (SEC)     0    0    0    0

 3  1246  035.9  85 07 25  09 25  MAX AMP  (M V)   853  975 1402  622  M
                                  DURATION (SEC)    50   67   53   50

    SUM- 38    *** AMP=SA-16 50* (CH.4 L4*100)  DELAY=SD-12  AZM=N X E

 1  1290  003.3  85 08 10  09 54  MAX AMP  (M V)   139  100  102  104  M
                                  DURATION (SEC)     0    0    0    0

 2  1310  046.0  85 08 19  18 26  MAX AMP  (M V)   131   63   65   73  M
                                  DURATION (SEC)     0    0    0    0

 3  1350  111.7  85 09 02  06 40  MAX AMP  (M V)    75  124   56   39  L
                                  DURATION (SEC)     0    0    0    0

 4  1365  158.9  85 09 05  01 11  MAX AMP  (M V)   114   60   80   46  N
                                  DURATION (SEC)     0    0    0    0

JEND
```

Fig. 8 An example of data lists selected with the following conditions; event group=$L(t_{s-p}<$ 7 sec), $M(t_{s-p}<15$ sec) and $N(t_{s-p}<30$ sec), maximum amplitude>100 mV, and excluding the events with imperfect initial motion and some recording troubles.

shows an example of the data set selected with this method. This is thought to be very useful for a seismometry dealing with a lot of data, such as a temporal observation of aftershocks.

4. Attenuation of seismic wave

Attenuation of seismic waves with distance is larger in the higher frequency range. Therefore, it is important to know the attenuation of S_g and L_g waves in the frequency range of 1–30 Hz for the study of ground vibrational characteristics. In this frequency range the scattering loss of energy is considered to play an important role in attenuation mechanism, because various heterogeneities are thought to exist in the lithosphere[19–23]. This consideration is based on the observational results that the attenuation property of S wave resembles that of coda wave in the frequency dependent characteristics[24,25].

Attenuation properties of coda waves and S waves from local small earthquakes occurring in and around the Kinki district were studied critically[3,26]. The results are as follows:

(1) Q_c, obtained by a functional form for coda decay, $t^{-a}e^{-bt}$, with $a=1$ and $Q_c=\pi f/b$, depends systematically on the frequency as well as on the lapse time measured from the source origin time.

(2) Q_c is approximated by $160\sqrt{f}$ for $20<t<60$ sec, and $230\sqrt{f}$ for $50<t<$ 200 sec.

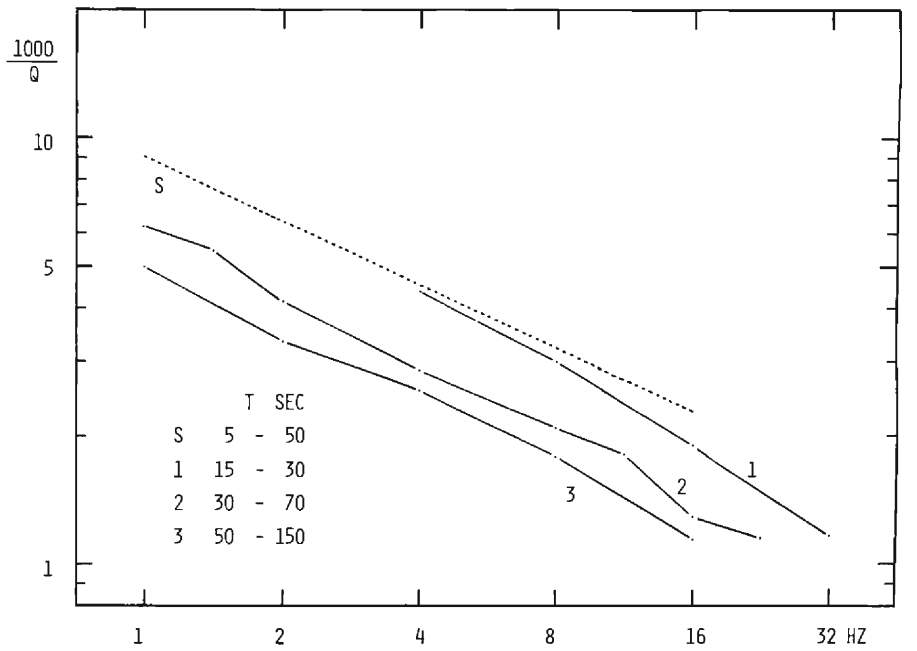

Fig. 9 Q_c^{-1} in various lapse time intervals and Q_s^{-1} for the Kinki district.

(3) The decrease of attenuation with lapse time was considered to reflect the layered Q-structure in the upper lithosphere.

(4) Q_s, obtained with the two different methods, shows the same frequency dependent property as Q_c.

(5) Q_s is approximated by $110\sqrt{f}$ for $5<t<50$ sec.

Fig. 9 shows Q_c^{-1} in the various lapse time intervals and Q_s^{-1}. It seems that Q_c^{-1} converges to Q_s^{-1} as the lapse time interval approaches the S travel time. The observation of the similar attenuation for S wave and coda wave suggests the same attenuation mechanism, that is, the scattering loss of energy in the frequency range of 1–30 Hz.

In the practical sense, the observation of $Q_c^{-1} \cong Q_s^{-1}$ avails to estimate the efective Q_s^{-1}, because the estimation of coda decay is easier with better accuracy compared to the direct measurement of Q_s^{-1} such as the spectral ratio method and the comparative examination of array data. The coda decay, moreover, can be examined without any assumptions about the dependency on frequency. However, Q_c^{-1} will reflect the wider and deeper area than Q_s^{-1}.

In our analysis, Q_c^{-1} was discussed with the averaged value of many events. However, Q_c^{-1} with a large lapse time intervla varies with source location and source depth. For example, Q_c^{-1} of the events in the central and southern parts of the Chubu district, the eastern adjacent district of the Kinki district, is larger by 20–30 % than that in the Inner Zone of the Kinki district, and Q_c^{-1} for the Outer Zone

is slightly larger than that for the Inner Zone. These regional variations are described in **Appendix 2.** Therefore our result, $Q_s=110\sqrt{f}$ is thought applicable for the crust in the Inner Zone of the Kinki district.

Okano and Hirano discussed the attenuation property of body waves in the crust in the vicinity of Kyoto with the spectral ratio method under an assumption of the constant Q[27]. However, their result may be equivalent to ours, if taking the assumption of $Q\propto\sqrt{f}$[3]. Umeda showed that the attenuation in the upper crust is relatively large[28]. Fedotov and Boldyrev studied the frequency dependent attenuation and its variation with depth[24]. Aki proposed the single station method for estimation of Q_s[25], and discussed the dependence of attenuations on frequency in relation to the tectonic activity of the lithosphere[29)-31]. Rautian *et al.* discussed the variation of Q_c with frequency and lapse time[32]. Their result is, in a wide frequency range of 0.2–40 Hz, $Q_c=360\sqrt{f}$ for $t=8$–200 sec and $Q_c=70\sqrt{f}$ for $t=2$–8 sec in the Garm region, the frequency and time dependent properties of which resemble those of our results. The attenuation of L_g wave was examined to be frequency dependent[33]. All these observations in many places suggest that Q_s^{-1} and Q_c^{-1} depend on frequency and depth systematically in the same manner.

Okano and Hirano suggested that the attenuation in the northern parts is small compared with that in the southern parts in the vicinity of Kyoto, and that the attenuation in the seismic zone is, as a whole, small for seismic waves propagating in the EW direction which coincides with the direction of the global tectonic force[34]. Our result of Q_s may average the possible regional and directional variation in the Kinki district.

Gusev and Lemzikov studied the variation of Q_c before large earthquakes in the Kurile–Kamchatka region[35]. At the present time, however, any temporal variations of Q_c are not visible in and around the Kinki district. Even if they exist, the amount of variation may be negligibly small.

From the above consideration we may conclude as follows: Q_c and Q_s vary with frequency and lapse time or travel time systematically in the same manner. Q_s is approximated by $110\sqrt{f}$ for the crust of the Inner Zone in the Kinki district in the frequency range of 1–30 Hz.

5. Regional variation of source property and its effects on vibrational characteristics

In the vicinity of Kyoto, the spectral contents of body waves from small and micro earthquakes have been investigated deterministically with Fourier analysis and discussed in relation to the seismic activity and stress in the crust[1,2,36]. Short period body waves will be affected significantly by the fine local geology and topography [37,38]. Therefore suitable smoothing or averaging processing are necessary.

In these ten years, extensive studies have estimated seismic coda to investigate the source problems of small earthquakes, utilizing the fact that the coda property

is regular even in the high frequency range of a few tens Hz. The method is based on the empirical rule that seismic coda is determined only by the source spectrum and the scattering property in the medium. However, the coda excitation must be calibrated by some body wave analysis, because the scattering process is not well elucidated.

We have discussed the regional variation of source spectra for small events with coda analysis[3]. In this section we summarize the results, and examine the vibrational characteristics of larger events recorded by **SMS** at **SUM** in relation to the regionality of stress suggested by coda analysis of smaller events.

The regional variation of seismicity in the Kinki district was explained briefly in §. **2** with **Figs. 2** and **3**.

5.1 M_o–f_c relation inferred from coda analysis[3]

The far-field displacement spectra of S waves were estimated with coda spectra for the small events in and around the Kinki district. Using the low frequency spectral level, U_0, and corner frequency, f_c, we evaluated the seismic moment, M_o, equivalent source radius, r, and stress drop, $\Delta\sigma$, with the Brune's model of dislocation[39,40] and the result of Keilis-Borok[41]. The relation between M_o and f_c is shown in **Fig. 10** and the locations of the sources are in **Fig. 11.** The slope of the constant stress drop line is -3 by definition. Some tendencies of the source properties and scaling law can be obtained: The M_o–f_c relation is much steeper than -3 in the range of $M_o<10^{21}$. As a result the amount of stress drop increases from a few bars to about 10 bars with increase of moment. In the range of $M_o>10^{21}$, however, the slope is nearly -3. The amount of stress drop varies with events from 10 to 100 bars.

In addition to the above general tendency for this area, it is very remarkable that the M_o–f_c relation varies systematically with source locations. That is, f_c of the shallow events near Wakayama (◎) (cf. **Fig. 2**(**A**)) and those in the seismic zone from Lake Biwa to Osaka Bay (○) (cf. **Fig. 3**) are lower than f_c of the events with the same M_o level in the other regions. Therefore the events in the regions of high seismic activity are characterized by relatively low stress drop. On the contrary the events in the Nara and Mie prefectures (△), which are known as a non-active region in seismicity, show high stress drop. The deeper events in this region (△) and the Yoshino region (▽) also show high stress drop. Although the events in and off the Kii peninsula and in the Kii channel (□), the southern parts of the Outer Zone, had a relatively large source depth of 40–60 km, the stress drops are smaller than those of the above mentioned deep events (△, ▽). Therefore we may arrive at the following conclusions: the stress drop in the Inner Zone is higher than that in the Outer Zone, and the stress drop becomes lower in the southernmost region in the Outer Zone.

The events near the Ontake–Volcano (Nos. 56 and 57, ⊕) show quite a different nature, that is, the high stress drop in spite of the high seismic activity in a swarm. In the analysis of spectral contents in the body waves, which was carried

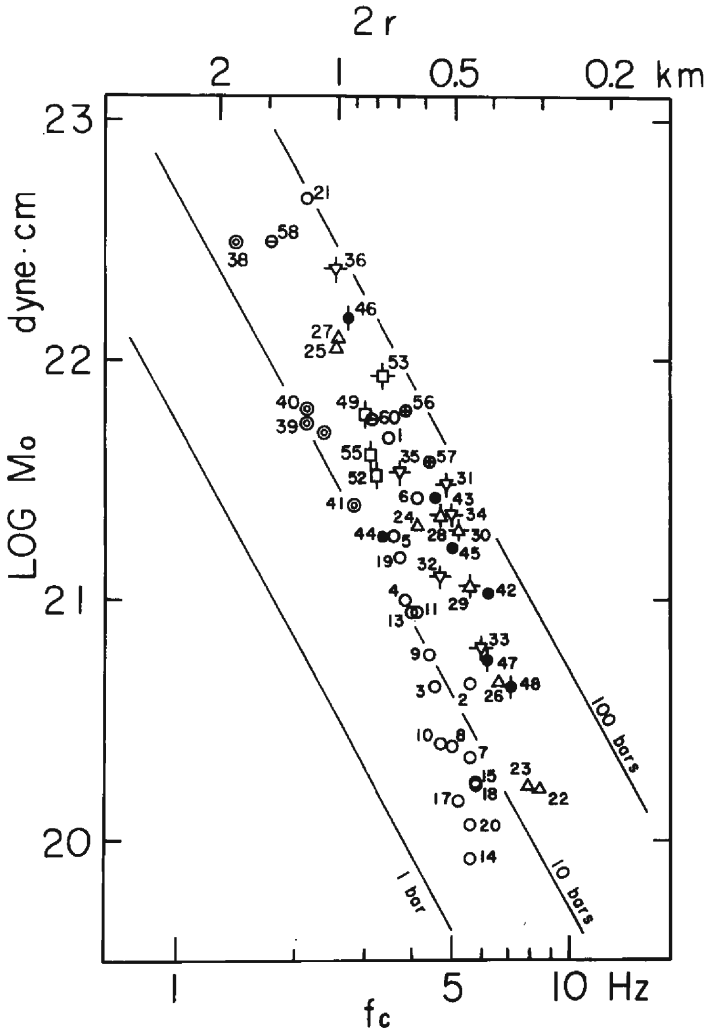

Fig. 10 M_o–f_c relations obtained by coda analysis for small events in and around the Kinki district. ○: near Kyoto, ◎: near Wakayama, △: Nara and Mie Prefectures (Iga-Ueno region), ▽: Yoshino region, ●: Aichi, Gifu and Mie Prefectures, □: Kii channel, in and off Kii Pen., ⊕: SW Nagano Prefecture, ⊖: others. The event numbers are the same as those in **Fig. 11** (Reproduction of **Fig. 15** in the previous pap.[3]).

out for the evaluation of attenuation, the high frequency components were very large compared with those of the other regions[3]. This earthquake swarm, occurring from August 1976, has attracted geophysical interest in connection with the abrupt eruption of the Ontake-Volcano on Oct. 28 1979[42]. It is also very interesting that the 1984 West Nagano Earthquake on Sept. 14 occurring in this region was characterized by an extremely large acceleration in the source area[43].

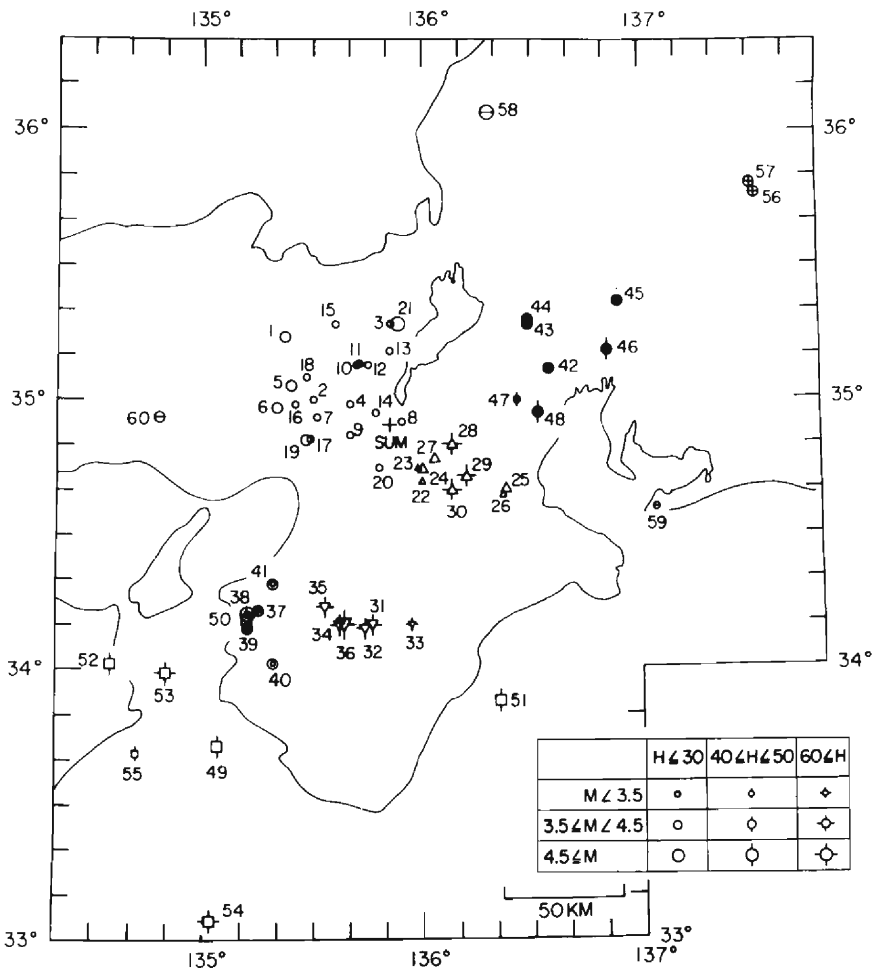

Fig. 11 Epicenters of the events used for coda analysis (Reproduction of Fig. 1 in the previous pap.[3]).

5.2 Variation of vibrational characteristics with source location

It is very interesting to know how the regionality of stress drop does or does not affect the vibrational process in the main vibrational parts during large earthquake. For this problem we have examined the seismograms of **SMS** at **SUM**. The source parameters of the events are listed in **Table 2.** **Fig. 12** shows the epicenters.

The transversal components of three events around the Kinki district are shown in **Fig. 13**. Comparing the wave forms, we can point out the characteristic feature as follows: Event No. 18, which is the smallest in magnitude, and deepest among the three, has the apparent predominant frequency of about 2 Hz, and the excitation of the crustal surface waves are very small. Event No. 26 has the predominant frequency of about 0.7 Hz. Event No. 37, which is the largest and shallowest among the three, is characterized by the large amplitude of high frequency in S_g

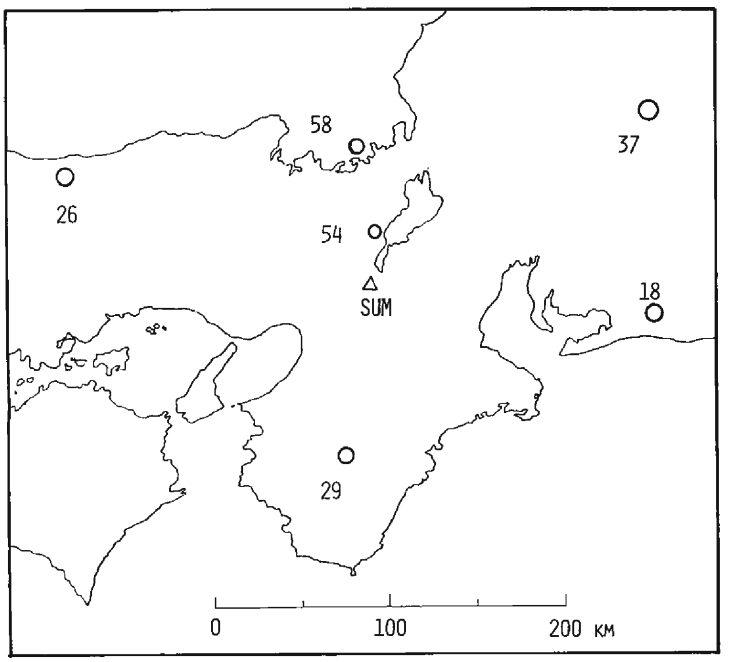

Fig. 12 Epicenters of the events used for response analysis.

Table 2 List of the events used for response analysis

NO	DATE Y	M	D	TIME H	M	LAT D	M	LONG D	M	DIST KM	H KM	AZM D	MAG
18	83	3	16	2	27	34	47.4	137	36.9	162	40	94	5.7
26	83	10	31	1	52	35	24.8	133	55.6	183	15	−72	6.2
29	84	2	11	4	49	34	2.8	135	43.3	97	67	−173	5.5
37	84	9	14	8	48	35	49.3	137	33.6	186	2	57	6.8
54	85	10	3	20	57	35	11.1	135	52.0	30	5	4	5.3*
58	85	11	27	9	2	35	37.2	135	44.3	79	7	−7	5.1**

* Determinde by the Regional Center for Earthquake Prediction, Faculty of Science, Kyoto University

** Determined by the Hokuriku Microearthquake Observatory, Disas. Prev. Res. Inst., Kyoto University

wave and the strong excitation of long period normal modes. The response spectra S_a and S_v are shown in **Fig. 14**. Although event No. 18 is smaller than No. 26, the peak values of S_a for No. 18 are larger than those of No. 26 in the frequency range above 1.5 Hz. The peak values of S_v are nearly the same regardless of the difference in the peak frequency. As the epicentral distances are not so different, the spectral features may be interpreted as the difference of stress drop. Event No. 37 occurred at the region where the stress drop was suggested to be high. The source depth is the shallowest among the events. From these conditions, the event may be characterized by the high frequency S_g waves and the strong excitation of normal modes.

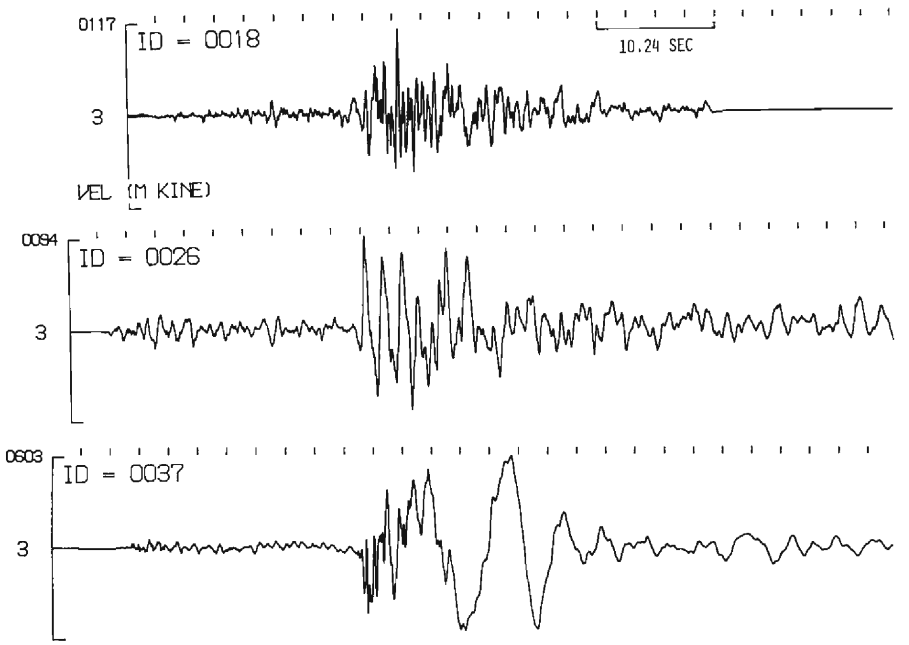

Fig. 13 Comparison of wave forms for the events around the Kinki district. Traces are transversal components of particle velocity in frequency range of 0.1–10 Hz.

In the Kinki district, we can also see the effect relating to the regionality of stress drop. The seismograms of the events with nearly the same magnitude are shown in **Fig. 15**, and the response spectra in **Fig. 16**. Event No. 29 occurring in the Yoshino region, shows the pulsive wave form and large response in the relatively high frequency range of 2–8 Hz. The Yoshino region was characterized by the high stress drop from the coda analysis. It is remarkable that event No. 54 is characterized by low frequency excitation below 1.5 Hz. This event occurred in the seismically active zone from Lake Biwa to Osaka Bay, and the source depth was the shallowest among the three. In this zone the stress drop was estimated lower than that in the other region by coda analysis. However, the very strong excitation in the frequency range below 1 Hz may not be explained only by the effect of the low stress drop peculiar to the region. Therefore the vibrational characteristics of event No. 54 may be considered to reflect the regional property of low stress drop as well as the shallow source depth.

On the contrary, event No. 58 is characterized by large excitation of high frequency contents from 5 Hz up to 25 Hz in S_a. It occurred on the north coastal region of the Kinki district. It was suggested that higher effective stress acts in the northern parts in the vicinity of Kyoto[1]. The location of the event No. 58 is somewhat apart from the region suggested. Therefore, the region with high stress may be extended to a more northern region in the Kinki district.

From the above consideration, the following conclusion may be obtainable:

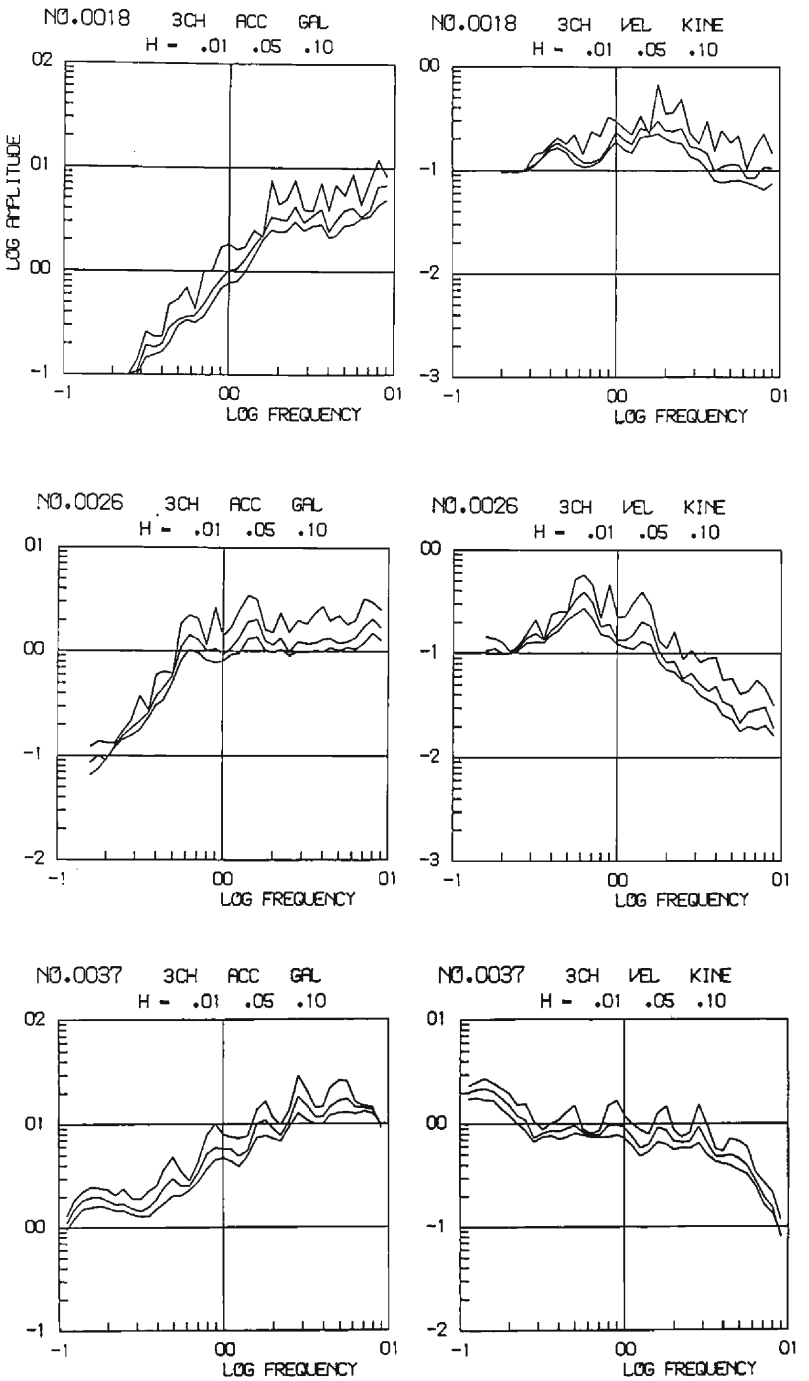

Fig. 14 Response spectra of S_a and S_v for the ground motion shown in **Fig. 13.**

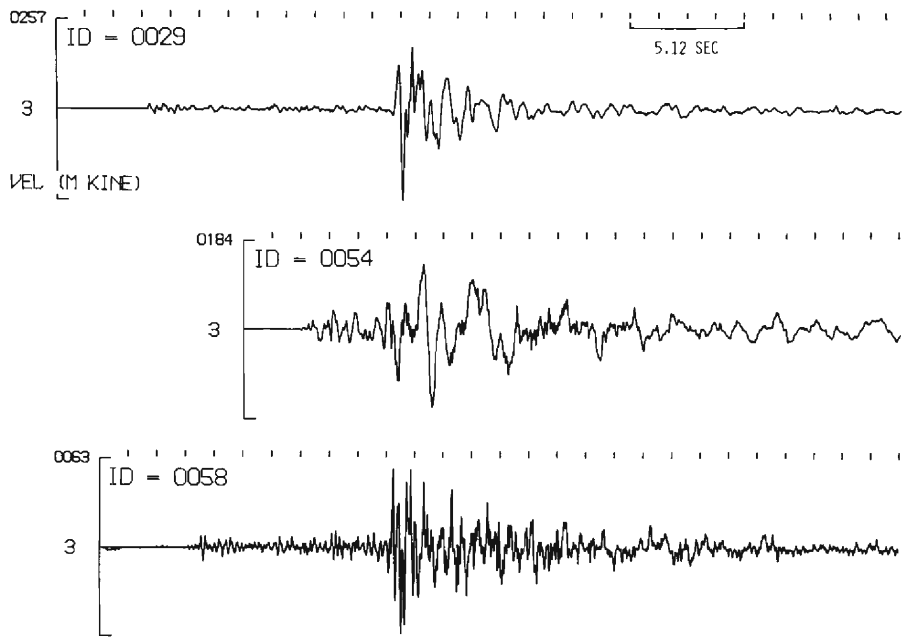

Fig. 15 Comparison of wave forms for the events in the Kinki district. Transversal componnets of particle velocity are shown in the frequency range of 0.25–25 Hz.

The vibrational characteristics of events with magnitudes of up to 7 reflect the stress property at the source region estimated by coda analysis of small events of $M<5$. The high frequency excitation of S_g wave is related to the source region with high stress drop. The strong excitation of low frequency range below 1 Hz correlates to source depths of shallower than 5 km.

6. Vibrational characteristics of soil ground in the Kyoto basin

The elucidation and prediction of vibrational characteristics for strong earthquake motion with periods of longer than 1 sec have grown into an important problem in engineernig seismology, because of rapid increase of structures with long natural periods, such as high rise buildings, long bridges and big storage tanks. In an urban area knowledge about the amplification of long period seismic waves by soil deposits is necessary. For this reason, predominant period and amplitude of long period microtremers were examined on soil grounds where the depth of bed rocks are over 100 m[eg. 5,44]. Appearance of spectral peaks for tremor at a soil ground depends on the velocity contrast between soil deposits and bed rock as well as the spectral contents of incident waves. It is well known that the microtremor in this frequency range is the "microseism" caused mainly by sea waves, and that both predominant frequency and amplitude change extremely depending on meteorological conditions in and around Japan[45,46]. The microseisms observed around Kyoto are considered

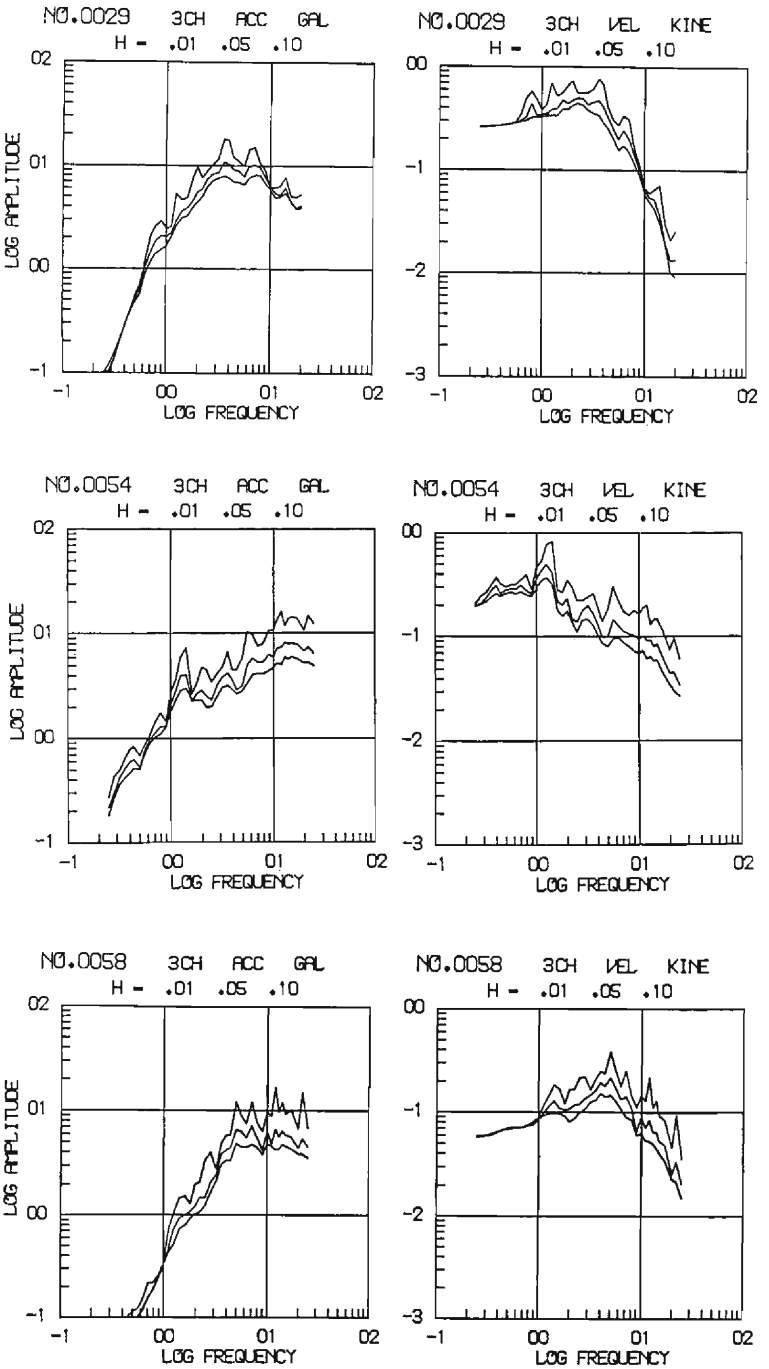

Fig. 16 Response spectra of S_a and S_v for the ground motion shown in **Fig. 15**.

to be composed of surface waves[47,48]. The long period components of strong motion seismograms are also considered to be surface waves[49]. Therefore the amplification of microseisms and their spatial variation could be a direct measure for seismic microzonation in an urban area. In the Kyoto basin the observation of microseisms were carried out at several ground sites with typical geological setting and at the adjacent rock site, **SUM**[6], and the amplifications for microseisms and for surface waves from near earthquakes were examined[7]. We summarize the results in this section.

The previous results were based on spectral features, therefore the details of the process of vibration during earthquake motion have not been clarified. In order to clarify the dynamic process in the characteristic frequency of the soil ground inferred from microseism, we examined the **SMS** seismograms of the 1984 West Nagano Prefecture Earthquake observed at **SUM** and the Seismic Station in the Uji Campus of Kyoto University (**GOK**).

6.1 Seismic amplification due to soil deposits inferred from microseism[6,7]

In order to examine the effects of soil deposits on microseisms, observations were carried out in the southern parts of the Kyoto basin and on the adjacent outcrop of the Paleozoic strata. The observational points and rough geological map are shown in **Fig. 17**. The basin is surrounded by the late Paleozoic complex consisting mainly of sandstone, slate and chart. The soil deposits are the Plio-Pleistocene Osaka Group with thin alluvial deposits and lie on the late Paleozoic basement. In the southeastern margin of the basin the Osaka Group forms mountain gravels and terraces.

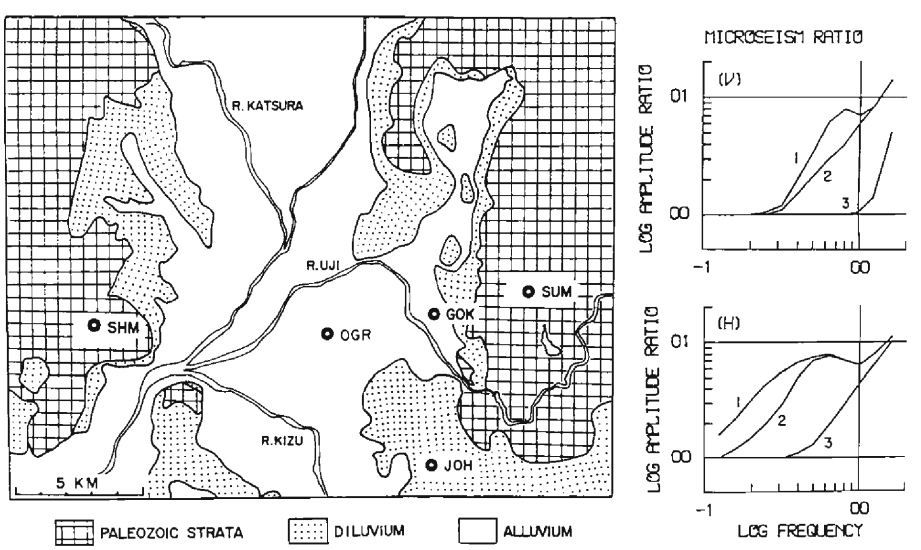

Fig. 17 Rough geological map of the southern parts of the Kyoto basin and the location of observationl points. Amplification factors due to the soil deposits inferred from microseism are shown, 1: OGR/SUM, 2: GOK/SUM and 3: JOH/SUM, respectively.

The seismic refraction investigation, carried out along an east-west line passing **GOK** and **OGR**, give a two layer velocity model: the soil layer with a velocity of 2.0–2.1 km/sec and the basement layer with a velocity of 4.4–5.2 km/sec; the configuration of basement layer is shaped like a ship bottom; the depth of the basement layer is approximately 700 m at **OGR** and 370 m at **GOK**[50,51]. The Seismic Station in the Uji Campus of Kyoto University is situated at **GOK**.

The following results were obtained through the spectral analyses:

The spectral features of microseisms such as peak frequency and peak amplitude at the ground sites as well as at the rock sites change remarkably according to the meteorological conditions. However, the averaged spectral ratio of microseisms at the ground site to that at the rock site shows a frequency dependent shape, which is almost invariant with time and is considered as an amplification factor of microseism due to soil deposits. The spectral ratio at each site is shown in **Fig. 17**. Amplification in the horizontal component is larger than that in the vertical one. The horizontal amplification begins to increase at lower frequency than the vertical one. The frequency of the peak amplification or the critical frequency at which amplification begins to increase become lower as a ground site moves from the environs to the center of the basin. The reliability of the estimated amplification can be checked with a standard deviation. In the Kyoto basin, for example, recordings of longer than 4 minutes should be repeated at least 6 times[52]. When the height of the significant sea waves along the Japan sea coast is over 1 m[53], the microseisms can be observed with a usual 1 sec seismometer with sufficient accuracy in the Kyoto basin.

6.2 Amplification of crustal surface waves from near earthquakes[7]

In order to discuss the applicability of the amplification factor inferred from microseism to the seismic amplification of earthquake motion, we examined the surface waves from near earthquakes with magnitudes of 5.7–6.8 and epicentral distances of 180–420 km, observed at **SUM** and **GOK**, through Fourier spectral analysis. The results are as follows: The peak frequency and peak amplitude in the spectral ratios (**GOK/SUM**) changed from event to event, however, the feature of the averaged ratio was nearly the same as the amplification factor of microseism shown in **Fig. 17** (cf. **Fig. 17** in the previous paper[7]). The amplification factor inferred from microseism is supposed to be an estimation of the maximum value of the seismic amplification for surface waves.

6.3 Long period vibrational characteristics during the 1984 West Nagano Prefecture Earthquake[8]

The 1984 West Nagano Prefecture Earthquake (M 6.8) observed by **SMS** at **SUM** was characterized by the large amplitude of high frequency S_g wave and the strong excitation of normal modes as discussed in §**5.2**. In order to see the dynamic process in the characteristic frequency of the soil ground inferred from microseism, we examined the **SMS** seismograms of the events. **Fig. 18** shows the three components (VRT) of the ground particle velocity at **SUM** and **GOK**. At the rock

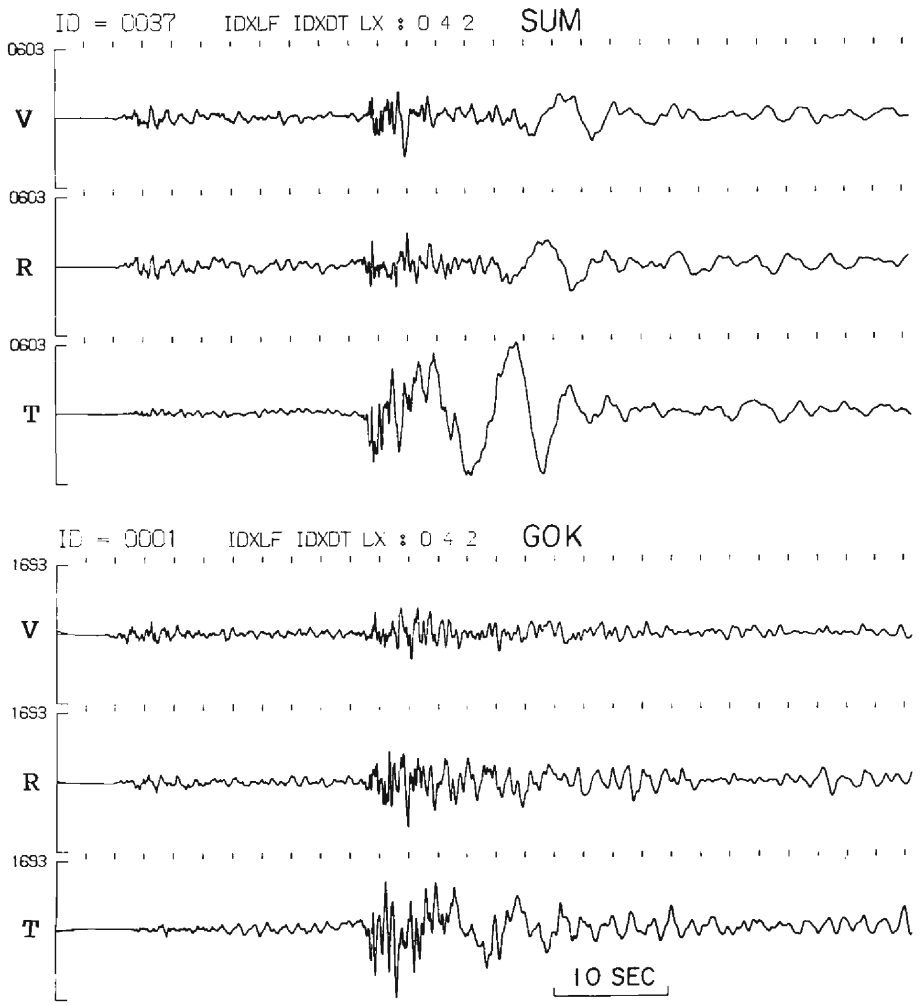

Fig. 18 Three components seismograms (VRT) of the 1984 West Nagano Prefecture Earthquake observed at **SUM** and **GOK**, showing particle velocity of ground with instrumental correction for frequency range of 0.1–10 Hz. The scale is in *m* kine.

site, **SUM**, following the high frequency S_g waves, the surface waves were extremely excited. The predominant periods are 4–5 sec for Rayleigh waves and 8 sec for Love waves. In order to clarify the frequency range of each wave group, the digital band pass filters were applied as shown in **Fig. 19**. In the vertical component at **SUM**, the three wave groups are distinguished; dispersive Rayleigh waves of fundamental mode (Band 2–6), pulsive S_n and S_g waves (Band 5–13) and surface waves of some higher modes (Band 4–9). In the transversal component, dispersive fundamental Love wave (Band 2–5), and S_g waves (Band 5–13) are separable. At the ground site, **GOK**, these wave groups are also recognized as a whole, though some interaction occurs in the intermediate frequency bands. In these bands each wave group was amplified and the duration was elongated. These bands correspond to

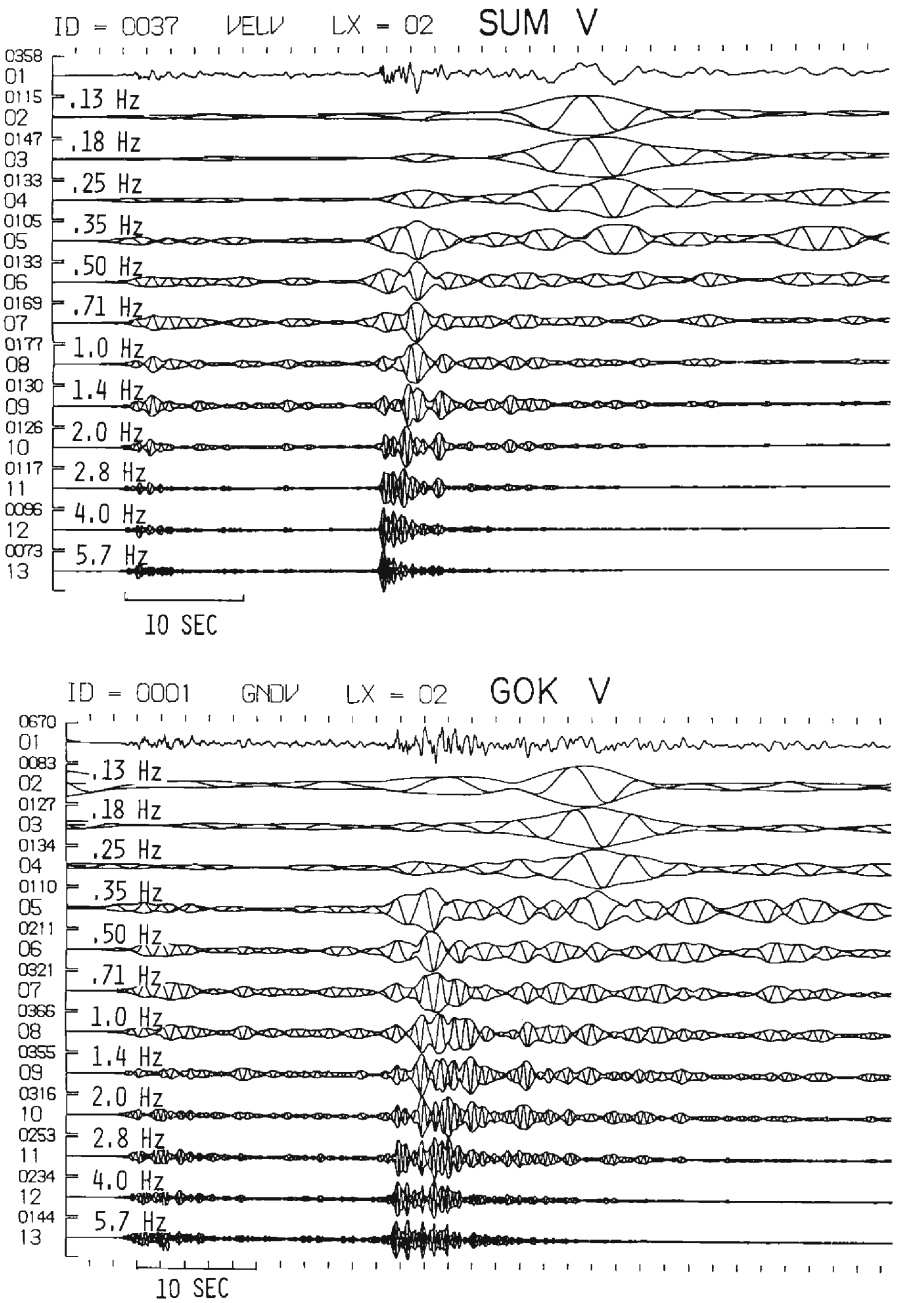

Fig. 19 Band-pass-filtered seismograms. Maximum amplitudes are shown above trace numbers in *m* kine. Trace 1 is particle velocity of 0.1–10 Hz.

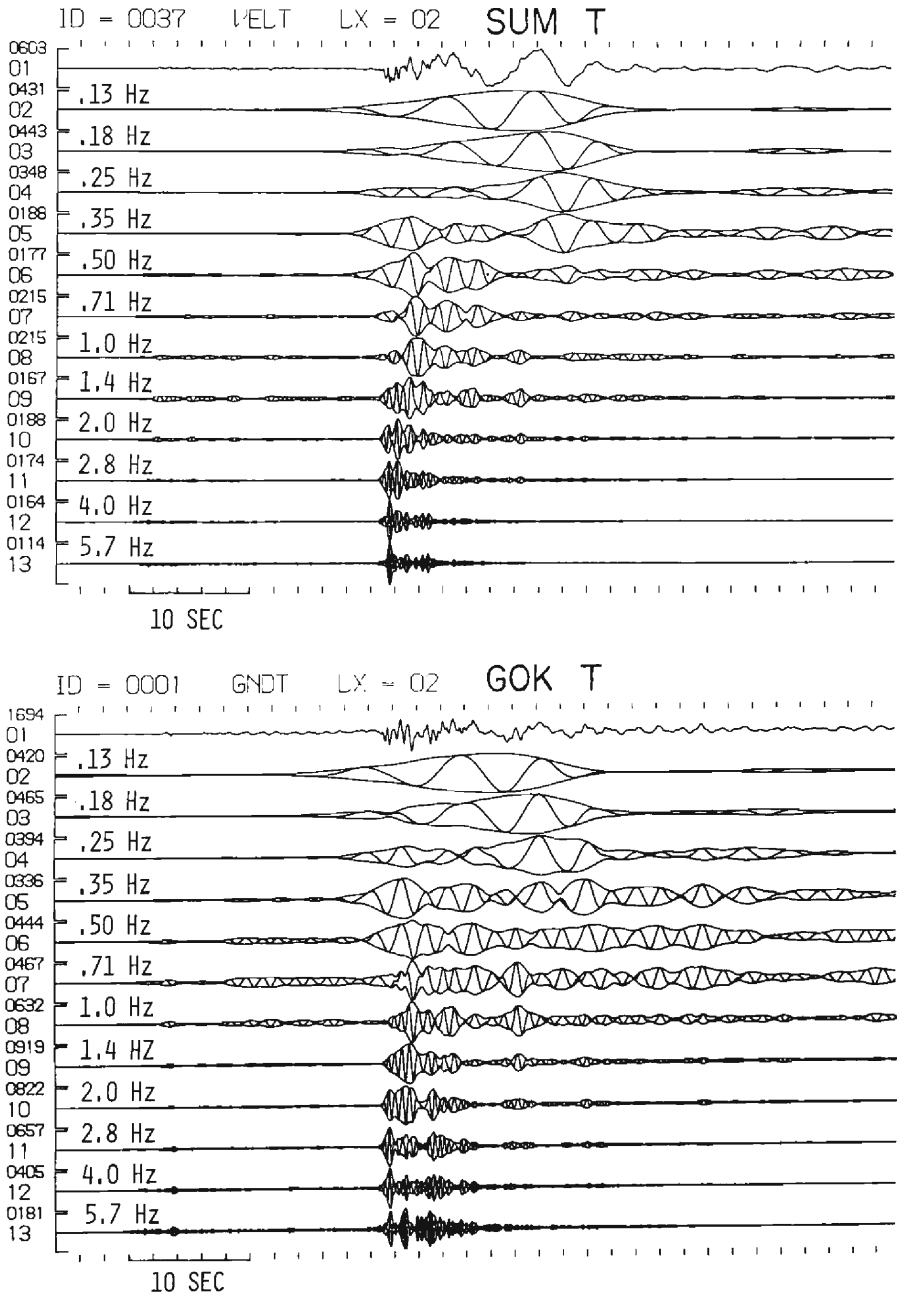

Fig. 19 (Continued) Band-pass-filtered seismograms. Maximum amplitudes are shown above trace numbers in m kine. Trace 1 is particle velocity of 0.1–10 Hz.

the characteristic frequency of the soil ground, **GOK**, inferred from microseism.

Fig. 20 shows the amplitude ratios of the envelopes for the corresponding wave groups (**GOK/SUM**). In the vertical component, the ratios of surface waves (△, □) increase from 1 at 0.3 Hz to 5 at 1 Hz, monotonically. In the horizontal component, the ratios of surface waves (△) have peak values of 5–7 at 0.7 Hz. Amplification for *S* waves are different from those for surface waves in the vertical and transversal components. In the radial component, it is somewhat difficult to distinguish the corresponding wave groups in the intermediate frequency range. However, the amplitude ratios of the surface wave groups are coincident with those of the transversal component[8]. From the above analysis it may be concluded that the effect of soil deposits during an earthquake motion is interpreted with the amplification and elongation of duration for each wave group and the resultant interference of wave groups in the characteristic frequency of the soil ground.

In order to see the effect of the interference, we examined the dynamic process by response analysis. In **Fig. 21** the velocity response spectra, S_v, of transversal components are shown with the symbols indicating the original wave groups which take the highest response in each frequency. In the frequency range of lower than 0.3 Hz, the spectral peaks are made by the fundamental Love wave. In the intermediate frequency range of 0.3–1.5 Hz, the two peaks are separable at **SUM**, while

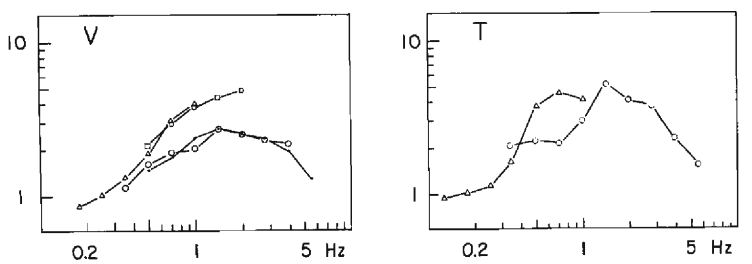

Fig. 20 Amplitude ratios of envelopes for typical wave groups. Dot: S_n, ○: S_g, △: fundamental Rayleigh or Love waves, □: higher mode between *S* and fundamental mode, respectively.

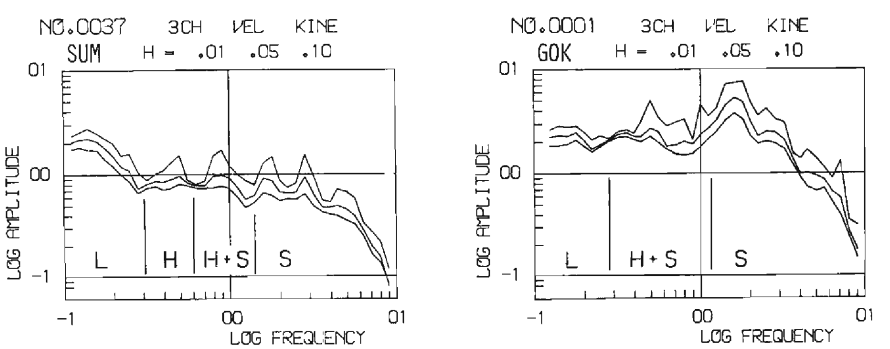

Fig. 21 Velocity response spectra of transversal components with h=0.01, 0.50 and 0.1. The wave groups making the spectral peaks are distinguished; *L*: fundamental Love wave, *H*: higher mode, *S*; S_g wave, respectively.

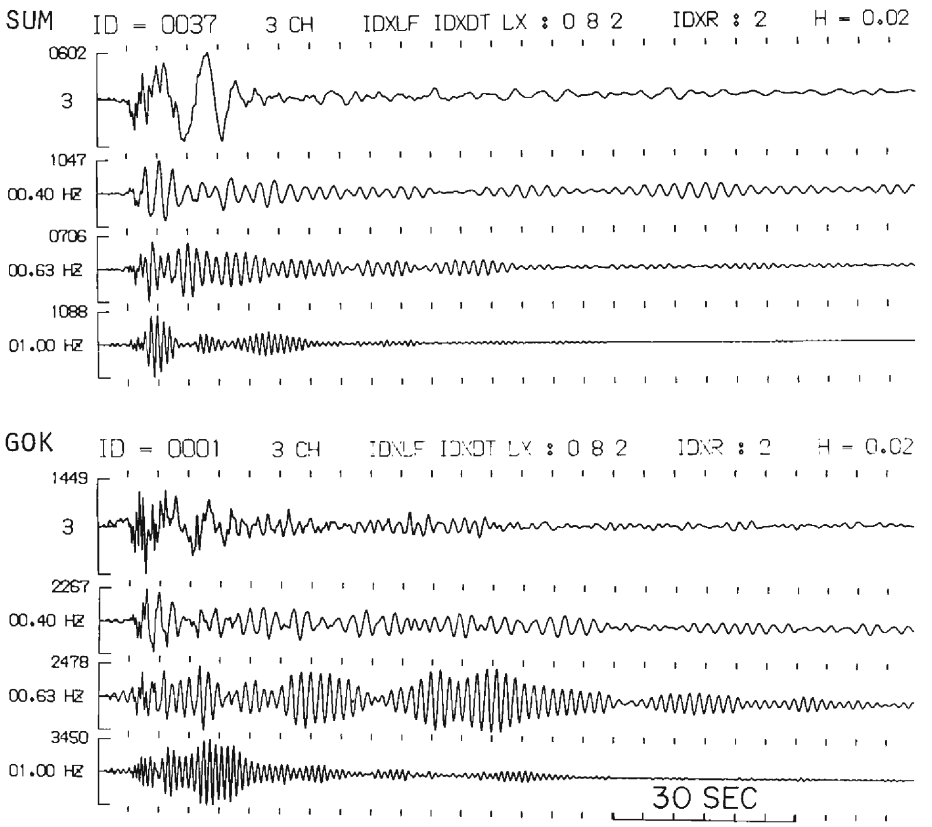

Fig. 22 Comparison of velocity responses of coda parts at **SUM** and **GOK** (h=0.02). The first trace in each site is the original seismogram of particle velocity.

not at **GOK**. These peaks are made by the interference of S_g wave and surface waves of higher modes in different manners between the sites, **SUM** and **GOK**. In the frequency range of higher than 1.5 Hz, the peaks are made by S_g waves at both sites. The dynamic process for constitution of the spectral peaks in the intermidiate frequency range is demonstrated with velocity responses of h=0.02 as shown in **Fig. 22**. It is remarkable that the vibration of 0.63 Hz increases with time and reachs to its maximum amplitude after 60 sec from the S arrival at **GOK**, while the vibration lasts only 20 sec at **SUM**. In this way the spectral peaks around the characteristic frequency of the soil ground may be formed. This example shows that the seismic coda plays an important role in the vibrational process according to the characteristic frequency of soil ground.

7. Discussion

The regional variation of stress drop and seismic wave attenuation were suggested from coda analysis in and around the Kinki district. The Inner Zone is

characterized by high stress drop, while the Outer Zone by low stress drop. The attenuation in the Inner Zone is smaller than that in the Outer Zone. It is very interesting that both regional variations must reflect their respective geological and tectonic states, because the geological age of the Outer Zone is considered to be younger than the Inner Zone and the tectonic activity is higher in the Outer Zone. The stress drop in each region may become higher with increase of source depth. The stress drop is low in the seismically active region, such as the zone from Lake Biwa to Osaka Bay, where micro earthquakes occur frequently, and the region near Wakayama, where many small events are occurring in a swarm. However, the source region of the 1984 West Nagnao Prefecture Earthquake near the Ontake-Volcano is exceptional, because the stress drop has been high in spite of high seismic activity from 1976.

From the point of view of the engineering seismology it is important to examine how the regionality of stress drop does or does not affect the vibrational process in the main vibrational parts during a large earthquake. For this reason the seismograms of **SMS** at **SUM** with magnitude of 5.1–6.8 were analyzed. The S_g waves from the events occurring in the probable high stress region were characterized by high frequency contents. In particular the shallow event No. 58 occurring at the coastal region of the Wakasa Bay on the northernmost Kinki district was remarkable in its high frequency excitation. Hirano suggested that higher stress is acting in the northern parts in the vicinity of Kyoto[1]. As mentioned previously, the high stress region may be extended to more northern parts. This regional variation of stress drop may reflect the property of the geological structure of the metamorphic Hida and Maizuru zones (**Fig. 1**). As discussed in **Appendix 2**, the coda decay for the Inner Zone including the above coastal region of the Wakasa Bay is smaller than that for the Outer Zone. It was also suggested that the attenuation in the northern parts is small compared with that in the southern parts in the vicinity of Kyoto[34]. Therefore it may be suggested that the vibrational characteristics due to the events occurring in the northern region tend to be characterized by high frequency excitation compared to that in the southern region of the Kinki district, and that large acceleration even by moderate earthquakes may be predicted in the northernmost region.

It must be pointed out that the seismograms of the 1984 West Nagano Prefecture Earthquake (M6.8), occurring in the region of high stress drop inferred from coda analysis of small events, were characterized by large amplitudes of high frequency components in S_g waves. In the source area the large acceleration of over a few g was estimated by the flight of many and various objects[43]. Therefore, it may be concluded that the coda analysis of small events of $M<5$ is useful for the study on the high frequency vibrational characteristics of large events. To put it in the concrete, the survey for regional seismic zoning[54] is necessary to evaluate the reginoality of stress drop, for which coda spectral analysis may be superior to spectral analysis of body waves, because the coda waves rule out the effects of the fine local geology and topography on the high frequency components.

In addition to the regional variation of stress drop, the source depth plays an important role in low frequency excitation. When the depth was shallower than about 5 km, the frequency components below 1 Hz were excited strongly and were likely to form the various crustal surface modes as shown by the events Nos. 37 and 54.

The vibrational characteristics and the process of vibration at the soil ground in the Kyoto basin were examined in comparison with those at the rock site, **SUM**, with use of the **SMS** seismograms of the 1984 West Nagano Prefecture Earthquake. The vibrational characteristics were interpreted in regard to the amplification effects by soil deposits which had been inferred from the observation of microseism in the frequency range of lower than 1 Hz. At the ground site, **GOK**, the characteristic frequency for the soil ground had been estimated to be around 0.63 Hz, and the amplification factor about 8 for the horizontal component. As the epicentral distance was relatively large (186 km for **SUM**), various wave groups were separable. The seismic amplification of the soil ground was observed in the combined process; amplification and elongation of duration for each wave mode, and interference of various modes in the characteristic frequency of the soil ground predicted by microseism. The amplitude ratio of the surfcae waves (ground/rock) was nearly the same as that of microseism. It was demonstrated that the vibration of seismic coda may act as a strong source of excitation for structures, when the damping of the structure is small and the natural frequency is near the characteristic frequency of the ground. From the above examination we are convinced that the observation of microseism is useful for the seismic microzonation in the basin, although there remain some problems to be discussed about the mode contents of microseism and earthquake motion and the mode conversion at the boundary of the basin. In practice it is very useful that microseisms can be observed with a usual 1-sec seismometer with sufficient accuracy, when the height of the significant sea waves along the Japan sae coast is over 1 m. This may be met usually in winter[53]. Means are also available to check the reliability of the amplification factor with the standard deviation for repeated observations[6,7].

As for the problems in seismometry, it was convinced that the **SYM** is superior to the usual system with a vertical and two horizontal seismometers in the accuracy and the reliability, particular in the frequency range lower than the seismometer's natural frequency, such as the range for the microseism and the L_g or R_g waves as discussed in this study. The application of the micro-processor technique and the utilization of the solid-state magnetic bubble memory for the strong motion seismometry proved to be very reliable along with easy maintenance.

8. Conclusion

The high frequency vibrational characteristics in the S_g waves from large earthquakes may reflect the regionality of the stress drop derived from coda analysis of

small events. Large acceleration even by moderate earthquakes may be predicted in the northernmost region in the Kinki district, where high stress and small wave attenuation have been suggested. The coda analysis of small events is very useful for elucidation and prediction of the vibrational characteristics for large earthquake, and is applicable to the regional seismic zoning concerning the regionality of stress drop.

As for the attenuation of seismic waves, the regional variation of coda decay was observed. Consequently our previous result concerning the S wave attenuation, $Q_s=110\sqrt{f}$, must be restricted to the crust in the Inner Zone in the Kinki district.

The vibrational process at the soil ground in the Kyoto basin was clarified in relation to the characteristic frequency of the ground inferred from microseism. The amplification effects of the soil ground were characterized by the amplification and the elongation of duration of each wave mode and the interference of the various modes in the characteristic frequency of the soil ground. The amplification factor of microseism was considered to give the maximum value of the amplification of the seismic surface waves in the frequency range of lower than about 1 Hz. Regional variation of amplification for microseism is considered to be the direct measurement for the microzonation of the soil ground in the basin.

Acknowledgement

The author wishes to express his sincere thanks to Prof. Soji Yoshikawa of Kyoto University for his encouragement in carrying out this work.

References

1) Hirano, I.: Source Characteristics of the Earthquakes Occurring in the Vicinity of Kyoto, Bull. Disas. Prev. Res. Inst., Kyoto Univ., Vol. 24, 1974, pp. 67–80.
2) Furuzawa, T., K. Irikura and J. Akamatsu: Regional Variation of Body Waves' Spectra from Local Small Earthquakes Occurring in the Southern Parts of Kyoto, Zishin, Ser. 2, Vol. 26, 1973, pp. 275–284 (in Japanese).
3) Akamatsu, J.: Attenuation Property of Seismic Waves and Source Characteristics of Small Earthquakes, Bull. Disas. Prev. Res. Inst., Kyoto Univ., Vol. 30, 1980, pp. 53–80.
4) Ohta, Y., H. Kagami, N. Goto and K. Kudo: Observation of 1- to 5-Second Microtremors and Their Application to Earthquake Engineering. Part 1., Bull. Seis. Soc. Am., Vol. 68, 1978, pp. 767–779.
5) Kagami, H., J. Horita, Y. Ohta, N. Sakajiri, A. Yoshida, A. Tanaka and A. Kubotera: Observation of 1- to 5-second Microtremors and Their Application to Earthquake Engineering. Part 8, Zishin, 2nd Ser., Vol. 36, 1983, pp. 609–617 (in Japanese).
6) Akamatsu, J.: Observation of Microseisms and Amplification of Surface Waves by Soil Deposits, Annuals of Disas. Prev. Res. Inst., Kyoto Univ., No. 26B–1, 1983, pp. 43–52 (in Japanese).
7) Akamatsu, J.: Seismic Amplification by Soil Deposits Inferred from Vibrational Characteristics of Microseism, Bull. Disas. Prev. Res. Inst., Kyoto Univ., Vol. 34, 1984, pp. 105–127.
8) Akamatsu, J.: Long Period Vibrational Characteristics of Soil Deposits in the Kyoto Basin During the Western Nagano Prefecture Earthquake, Annuals of Disas. Prev. Res. Inst., Kyoto Univ., No. 28 B–1, 1985, pp. 21–29 (in Japanese).

9) Akamatsu, J. and M. Nishi: On the Seismic Observation with a Symmetrical Three- Component Seismograph System, Annuals of Disas. Prev. Res. Inst., Kyoto Univ., No. 22 B-1, 1979, pp. 83–90.
10) Akmaatsu, J.: A Digital Strong Motion Seismograph System Utilizing Magnetic Bubble Memory, Annuals of Disas. Prev. Res. Inst., Kyoto Univ., No. 25 B-1, 1982, pp. 1–9.
11) Akamatsu, J., T. Furuzawa and K. Irikura: On Nature of S Waves from Local Small Earthquakes Observed at Amagase Crustal Movement Observatory, Annuals of Disas. Prev. Res. Inst., Kyoto Univ., No. 18B, 1975, pp. 11–21.
12) Akamatsu, J.: Seismic Observation at the Sumiyama Seismic Station—On Nature of Ground Particle Motions of Seismic Waves from Local Small Earthquakes—, Annuals of Disas. Prev. Res. Inst., Kyoto Univ., No. 20 B-1, 1977, pp. 13–19.
13) Geological Survey of Japan: Geology and Minearl Resources of Japan 3rd Edit., 1977, Sumitomo Print. & Pub., pp. 6–10.
14) Geological Survey of Japan: Geological Structure, The National Atlas of Japan, 1976.
15) Maeda, N. and H. Watanabe: Mode of Activity of Microearthquakes —In the Case of the Middle and Northern Parts of Kinki District, Southwestern Japan—, Zishin, ser. 2, Vol. 37, 1984, pp. 579–598 (in Japanese).
16) Furuzawa, T.: Some Froblems of Seismic Data Processing, Part 1, Bull. Disas. Prev. Res. Inst., Kyoto Univ., Vol. 24, 1974, pp. 49–66.
17) Galperin, E.I.: Polarization Method of Seismic Exploration, Nedra Press, Moscow, 1977, pp. 56–62 (in Russian).
18) Furuzawa, T. and J. Akamatsu: On Remarkable Phases Observed between P and S waves from Local Small Earthquakes, Annuals of Disas. Prev. Res. Inst., Kyoto Univ., No. 21B-1, 1978, pp. 97–106 (in Japanese).
19) Nikolayev, A.V.: Seismic Properties of Weakly Heterogeneous Media, Izv., Earth Physics (English translation), 1968, pp. 481–487.
20) Aki, K.: Scattering of P Waves under the Montana Lasa, J. Geophys. Res., Vol. 78, 1973, pp. 1334–1346.
21) Aki, K.: Analysis of the Seismic Coda of Local Earthquakes as Scatterd Waves, J. Geophys. Res., Vol. 74, 1969, pp. 615–631.
22) Aki, K. and B. Chouet: Origin of Coad Wave; Source, Attenuation, and Scattering Effects, J. Geophys. Res., Vol. 80, 1975, pp. 3322–3342.
23) Tsujiura, M.: Spectral Analysis of the Coda Waves from Local Earthquakes, Bull. Earthquake Inst., Univ. of Tokyo, Vol. 53, 1978, pp. 1–48.
24) Fedotov, S.A. and S.A. Boldyrev: Frequency Dependence of the Body-Wave Absorption on the Crust and the Upper Mantle of the Kurile-Island Chain, Izv., Earth Physics (English translation), 1969, pp. 553–562.
25) Aki, K.: Scatterring and Attenuation of Shear Waves in the Lithosphere, J. Geophys. Res., Vol. 85, 1980, pp. 6496–6504.
26) Akamatsu, J.: Attenuation Property of Coda Parts of Seismic Waves from Local Earthquakes, Bull. Disas. Prev. Res. Inst., Kyoto Univ., Vol. 30, 1980, pp. 1–16.
27) Okano, K. and I. Hirano: Seismic Wave Attenuation in the Vicinity of Kyoto, Bull. Disas. Prev. Res. Inst., Kyoto Univ., Vol. 21, 1971, pp. 99–108.
28) Umeda, Y.: A Study on Attenuation of Seismic Waves in the Vicinity of Matsushiro (I)., Zishin, Ser. 2, Vol. 21, 1968, pp. 169–177 (in Japanese).
29) Roecker, S.W., J. King and D. Hatzffld: Estimation of Q in Central Asia as a Function of Frequency and Depth Using the Coda of Locally Recorded Earthquakes, Bull. Seis. Soc. Am., Vol. 72, 1982, pp. 129–149.
30) Biswas, N.N. and K. Aki: Characteristics of Coda Waves: Central and Southcentral Alaska, Bull. Seis. Soc. Am., Vol. 74, 1984, pp. 493–507.
31) Jin, A., T. Cao and K. Aki: Regional Change of Coda Q in the Oceanic Lithosphere, J. Geophys. Res., Vol. 90, 1985, pp. 8651–8659.
32) Rautian, T.G. and V.I. Khalturin: The Use of Coda for Determination of the Earthquake Source Spectrum, Bull. Seis. Soc. Am., Vol. 68, 1978, pp. 923–948.

33) Campillo, M., J.L. Plantet and M. Bouchon: Frequency-Dependent Attenuation in the Crust beneath Central France from Lg Waves: Data Analysis and Numerical Modeling, Bull. Seis. Soc. Am., Vol. 75, 1985, pp. 1395–1411.
34) Okano, K. and I. Hirano: Seismic Attenuation in Relatino to the Tectonic Force in the Vicinity of Kyoto, Bull. Disas. Prev. Res. Inst., Kyoto Univ. Vol. 22, 1973, pp. 97–110.
35) Gusev, A.A. and V.K. Lemzikov: The Anomalies of Small Earthquake Coda-Wave Characteristics before the Three Large Earthquakes of the Kurile-Kamchatka Zone, Volcanology and Seismology, No. 4, 1984, pp. 76–90 (in Russian).
36) Furuzawa, T.: Some Problems of Seismic Data Processing. Part 2, Bull. Disas. Prev. Res. Inst., Kyoto Univ., Vol. 24, 1974, pp. 127–145.
37) Furuzawa, T., S. Takemoto, K. Irikura and J. Akamatsu: Local Crustal Effects on Earthquake Seicmograms, Annuals Disas. Prev. Res. Inst., Kyoto Univ., No. 14A, 1971, pp. 189–202 (in Japanese).
38) Nishimura, K. and W. Morii: An Observed Effect of Topography on Seismic Ground Motions, Bull. Disas. Prev. Res. Inst., Kyoto Univ., Vol. 34, 1984, pp. 203–214.
39) Brune, J.N.: Tectonic Stress and the Spectra of Seismic Shear Waves from Earthquakes, J. Geophys. Res., Vol. 75, 1970, pp. 4997–5009.
40) Brune, J.N.: Correction, J. Geophys. Res., Vol. 76, 1971, p. 5002.
41) Keilis-Borok, V.I.: Investigation of the Mechanism of Earthquakes, Trudy Inst. Geofis. Akad. Nauk., SSSR, No. 40, 1957 (in Russian), English Transl., Soviet Res. Geophys. Ser., Vol. 4, 1960.
42) Mikumo, T., M. Koizumi and H. Wada: Seismicity, Focal Mechanism, and Tectonics in the Northern Hida Region, Central Japan, Zishin ser. 2, Vol. 38, 1985, pp. 25–40 (in Japanese).
43) Kuroiso, A., K. Ito, Y. Iio, Y. Umeda and I. Muramatsu: Surveys for Surface Ruptures and a High Acceleration Area of the Western Nagano Prefecture Earthquake of September 14, 1984, Annuals of Disas. Prev. Res. Inst., Kyoto Univ., No. 28B-1, 1985, pp. 171–184 (in Japanese).
44) Naruse, S., A. Yoshida, K. Masaki, H. Kagami, M. Miyazaki and A. Kubotera: Observation of 1- to 5-sec Microtremors and Their Application to Earthquake Engineering. Part 11, Zishin, Ser. 2, Vol. 37, 1984, pp. 383–395 (in Japanese).
45) Kagami, H., J. Horita, Y. Ohta, N. Sakajiri, A. Yoshida, A. Tanaka and A. Kubotera: Observation of 1- to 5-sec Microtremors and Their Application to Earthquake Engineering. Part 8, Zishin, Ser. 2, Vol. 36, 1983, pp. 609–617 (in Japanese).
46) Nesterov, V.A.: Stormy Microseisms in Shikotan Island and Water Pressure Fluctuations on the Pacific Ocean Floor, Volcanology, No. 2, 1982, pp. 73–79 (in Russian).
47) Okano, K.: Observational Study on Mkcroseisms (Part I), Bull. Disas. Prev. Res. Inst., Kyoto Univ., No. 44, 1961, pp. 2–22.
48) Oknao, K.: Observational Study on Microseisms (Part 2), Bull. Disas. Prev. Res. Inst., Kyoto Univ., No. 47, 1961, pp. 2–15.
49) Mamula, L., K. Kudo and E. Shima: Distribution of Ground-Motion Amplification Factors as a Function of Period (3–15 sec), in Japan, Bull. Earthquake Res. Inst., Univ. of Tokyo, Vol. 59, 1984, pp. 467–500.
50) Kitsunezaki, C., N. Goto and Y. Iwasaki: Underground Structure of the Southern Part of the Kyoto Basin Obtained from Seismic Explosion and Some Related Problems of Earthquake Engineering, Annuals of Disas. Prev. Res. Inst., Kyoto Univ., No. 14-B, 1971, pp. 203–215 (in Japanese).
51) Japanese National Committee for Upper Mantle Project: The Crust and Upper Mantle of the Japanese Area Part II, 1973, Geological Survey of Japan, Kawasaki.
52) Edit. Medvedev, S.V.: Seismic Microzonation, Nauka, Moscaw, 1977, pp. 67–75 (in Russian).
53) Tsuchiya, Y., M. Yamaguchi and H. Hiraguchi: Prediction of Ocean Wind Waves with Winter Monsoon on the Japan Sea, Annuals of Disas. Prev. Res. Inst,. Kyoto Univ., No. 26B-2, 1983, pp. 599–635 (in Japanese).
54) Edit. Medvedev, S.V.: Seismic Zoning of the USSR, Nauka, Moscaw, 1968, English Transl., Israel Program for Scientific Transl., Jerusalem, 1976.

55) Hagiwara, T.: Measurement of Vibration, Reprint, Hobunkan, Tokyo, 1971, pp. 135–142.
56) Willmore, P.L.: The Application of the Maxwell Impedance Bridge to the Calibration of Electromagnetic Seismographs, Bull. Seis. Soc. Am., Vol. 49, 1959, pp. 99–114.
57) Espinosa, A.F., G.H. Sutton and H.J. Miller, S.J.: A Transient Technique for Seismograph Calibration, Bull. Seis. Soc. Am., Vol. 52, 1962, pp. 767–779.

Appendix 1. Equation of motion for an inclined seismometer and the method of calibration

The equation of motion for an inclined pendulum is given by Hagiwara[55]. Taking the coordinate as shown in **Fig. A1–1**, we obtain the following equation from his eq. (32.14);

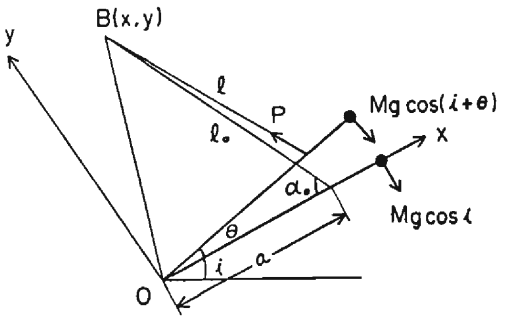

Fig. A1–1 Co-ordinate for inclined seismometer.

$$I\frac{d^2\theta}{dt^2} = -\beta a\left[(1-k)\frac{ay^2}{l_0^2}+k(x-y\tan i)\right]\theta + \frac{3\beta a^2 y}{2l_2^0}(1-k)\left(x-\frac{ay^2}{l_0^2}\right)\theta^2+0[\theta^3] \qquad \text{(A1–1)}$$

, where I: moment of inertia of pendulum, β: elastic constant of spring, a: distance between the center of rotation and the point of suspension by spring, k: a constant given by $k=1-l_0'/l_0$, and l_0': initial length of spring without load, l_0: spring length of the state of balance. The coefficient of θ^2 must be zero for simple harmonic oscillation, that is, (1) $k=1$ (zero length spring), (2) $\alpha_0=90°$ and (3) $\angle B=90°$. In our case the condition of $\alpha_0=90°$ is used, which is equivalent to the Gray type of horizontal pendulum. The period, T, is given by

$$T=2\pi\sqrt{\frac{I}{\beta a(a-kl_0\tan i)}} \qquad \text{(A1–2)}$$

The value of kl_0 is the extension of spring and varies inversely relative to the length, a. Therefore we may obtain a given period according to the point of suspension by the spring. In our routine observation at **SUM**, T is controlled to be 1 sec.

A relative frequency response for a seismometer with a moving coil can be examined precisely with calibration signals through a Maxwell bridge[56]. In our routine

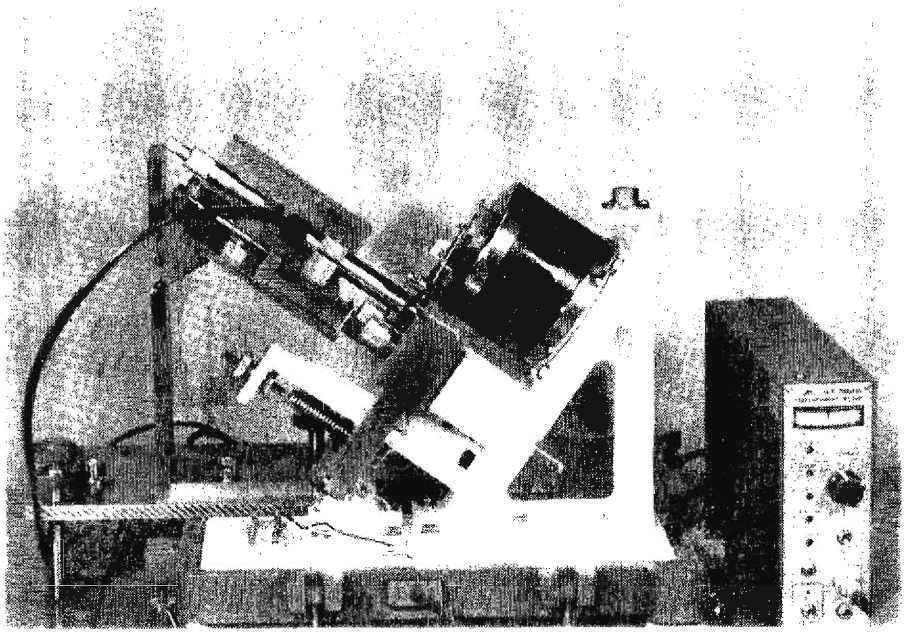

Photo. A1-1. The inclined seismometer with the probe of the displacement meter for mass movement.

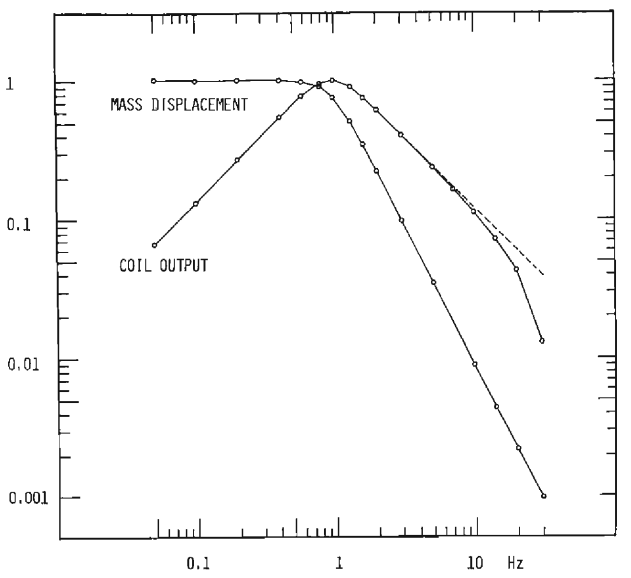

Fig. A1-2 An example of calibration with constant current of sine waves. The bridge was balanced at 1 Hz. Note that the output of coil becomes lower than theoretical curve (broken line) above 7 Hz, while the displacement of mass coincides with theoretical curve over a wide range of 0.05–30 Hz.

seismometry, however, the Wheatstone bridges are used instead of the Maxwell ones for simplicity[57] as shown in **Fig. 4**. This makes the response lower than the theoretical one in the high frequency range.

For the absolute calibration of the electro-magnetic constant, the motion of mass and the electrical current must be examined simultaneously. For this, we take an accurate measurement of the mass movement with a displacement meter, which utilizes the electric capacity between the pendulum and the probe of the meter fixed on the base. **Photo A1–1** shows the state of the measurement. **Fig. A1–2** shows an example of the result, from which it is noticed that the response obtained through the Wheatstone bridge is incorrect in the frequency range above 7 Hz. The actual displacement of mass fits fairly well to the theoretical curve in a wide frequency range of 0.05–30 Hz. The discrepancy above 7 Hz is due to the break of bridge balance and the real response through the coil is considered to be the same as the theoretical one.

Appendix 2. Regional variation of Q_c^{-1}

In the course of examination for the coda stability, the following regional variation of Q_c^{-1} was obtained. **Fig. A2–1** shows the epicenters of the events analyzed, and the source data are listed in **Table A2–1**. The events were grouped as follows:

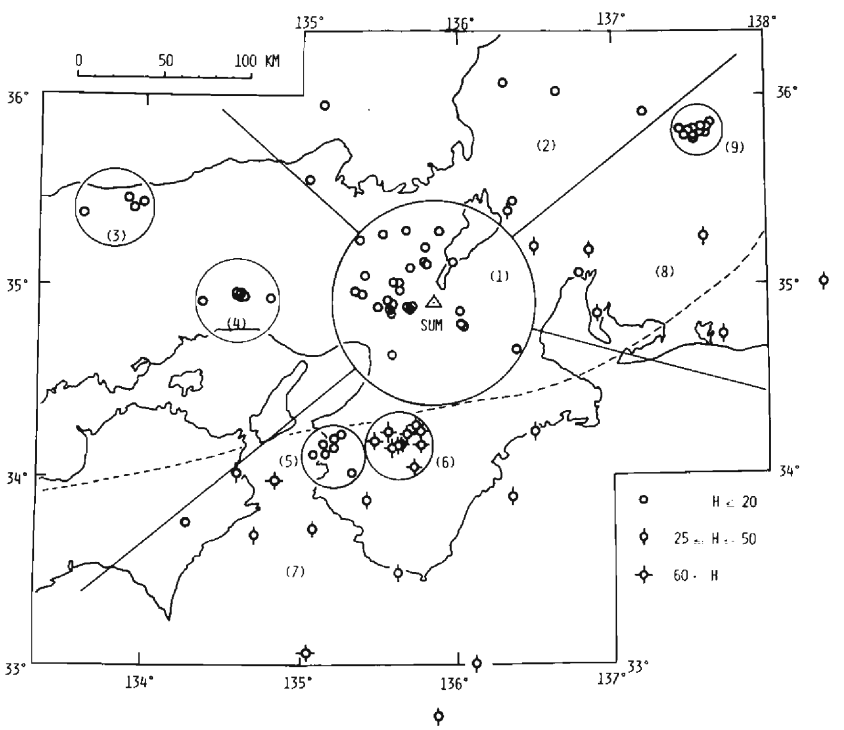

Fig. A2–1 Epicenters and grouping of the events analyzed for coda decay.

Table A2–1 List of the events analyzed for coda decay

NO	DATE Y	M	D	TIME H	M	LAT D	M	LONG D	M	D KM	H KM	AZM D	MAG
REGION 1													
1	76	9	14	21	42	35	14	135	22	56	10	−51	4.2
2	77	11	25	12	53	35	3	135	24	43	10	−70	3.8
3	78	1	7	6	1	34	58	135	20	47	10	−83	4.0
4	78	12	5	8	24	34	40	136	23	56	0	119	4.3
5	79	4	12	13	59	34	47	136	3	24	10	128	4.3
6	79	10	16	7	46	35	17	135	53	41	10	5	4.9
7	80	3	16	11	39	34	57	135	23	42	10	−84	3.4
8	80	3	24	10	49	35	16	135	31	49	0	−37	4.2
9	80	6	23	2	29	34	51	135	34	27	10	−105	2.8
10	80	9	11	20	46	35	8	135	58	27	20	24	4.6
11	81	1	19	9	44	34	54	135	35	24	10	−94	2.8
12	81	2	3	18	25	34	53	135	29	33	10	−96	3.8
13	81	2	19	15	51	35	1	135	35	27	10	−64	2.9
14	81	4	18	23	46	34	53	135	34	26	10	−98	2.8
15	83	11	16	5	13	35	1.0	135	37.6	23.0	17	−60	3.8
16	84	5	5	2	12	34	53.4	135	41.5	14.3	13	−101	4.6
17	84	5	19	16	39	34	52.4	135	40.7	15.9	9	−106	2.7
18	84	5	27	15	29	34	53.8	135	42.3	13.0	15	−98	3.0
19	84	6	25	2	3	35	6.7	135	48.6	22.0	16	−8	4.3
20	84	6	25	2	12	35	7.3	135	47.1	23.7	15	−13	3.0
21	84	7	5	1	24	34	52.1	136	1.0	16.4	10	108	2.8
22	84	7	7	19	48	34	47.8	136	1.3	20.7	10	129	2.8*
23	84	7	14	22	28	34	38.2	135	34.7	39.3	13	−141	2.8
24	84	7	17	1	49	34	51.7	135	34.4	25.5	14	−103	3.6
25	84	7	22	9	45	34	55.0	135	32.5	27.8	10	−89	3.5
26	84	8	7	17	43	34	52.8	135	40.3	16.3	13	−103	3.5
27	84	8	19	5	3	34	52.8	135	40.4	16.2	14	−103	3.0
28	84	10	1	19	19	34	58.3	135	37.7	20.9	13	−72	2.8
29	84	11	10	5	18	35	5.7	135	41.9	24.2	9	−34	2.7
30	84	12	2	19	8	35	17.0	135	40.6	43.8	7	−21	3.9
31	85	5	13	8	43	35	12.0	135	47.8	32.1	14	−8	3.4
REGION 2													
1	78	4	3	11	4	36	4	136	18	134	10	18	4.7
2	83	4	24	17	8	35	56.9	135	8.1	132	4	−29	3.9
3	83	10	6	14	21	35	55.0	137	12.5	166	0	48	4.5
4	83	12	29	13	10	35	33.3	135	2.6	102	7	−46	3.8
5	84	11	8	7	21	35	23.7	136	19.8	69	36	39	3.6
6	84	11	24	12	17	35	26.6	136	21.4	75	15	38	3.6
7	85	5	20	8	41	36	1.5	136	38.1	143	7	30	4.1

Table A2–1 (continued)

NO	DATE Y	M	D	TIME H	M	LAT D	M	LONG D	M	D KM	H KM	AZM D	MAG
REGION 3													
1	83	10	31	1	52	35	24.8	133	55.6	183	15	−72	6.2
2	83	10	31	1	55	35	26.2	133	59.5	179	13	−71	5.7
3	83	11	3	21	58	35	27.5	133	53.8	188	11	−71	4.8
4	85	7	2	13	21	35	22.5	133	36.8	210	14	−75	4.9
REGION 4													
1	79	10	13	16	30	34	56	134	48	96	10	−88	4.3
2	79	12	28	23	54	34	55	134	22	135	20	−89	4.9
3	84	5	30	12	42	34	56.7	134	36.5	113	18	−88	4.0
4	84	5	30	20	44	34	56.5	134	38.0	111	16	−88	4.0
5	84	5	30	22	32	34	57.0	134	36.2	114	15	−88	4.0
6	84	6	2	16	12	34	57.7	134	35.4	115	18	−87	4.3
7	84	6	5	13	48	34	56.9	134	35.8	114	16	−88	4.0
8	84	7	1	8	3	34	56.5	134	36.6	113	15	−88	3.9
REGION 5													
1	76	12	27	10	49	34	13	135	15	95	0	−145	4.0
2	77	8	7	4	27	34	12	135	12	99	0	−143	4.5
3	77	8	17	0	32	34	9	135	12	103	0	−145	4.0
4	79	4	17	20	26	34	1	135	19	111	0	−154	4.2
5	84	6	25	20	52	34	10.5	135	7.5	105	6	−141	4.4
6	85	4	14	16	24	34	7.1	135	4.1	114	9	−141	4.0
7	85	4	29	16	43	34	7.4	135	8.9	109	8	−144	4.1
REGION 6													
1	76	8	5	15	47	34	16	135	44	73	70	−172	4.2
2	76	12	21	8	4	34	10	135	46	83	60	−175	4.0
3	79	3	16	10	36	34	10	135	37	86	60	−166	4.0
4	79	7	31	9	3	34	14	135	33	80	70	−160	4.0
5	79	11	13	0	42	34	10	135	38	85	70	−167	4.8
6	83	7	18	9	21	34	14.2	135	45.8	76	64	−174	4.7
7	83	9	8	13	3	34	11.2	135	27.5	88	71	−156	4.0
8	84	2	11	4	49	34	2.8	135	43.3	97	67	−173	5.5
9	84	5	31	2	8	34	9.1	135	34.2	88	73	−163	3.9
10	85	5	3	1	1	34	13.7	135	40.7	78	72	−169	4.0
REGION 7													
1	76	7	18	15	30	33	43	135	4	151	40	−151	4.3
2	76	11	11	6	5	34	14	136	30	97	40	141	4.4
3	77	9	8	18	13	33	45	134	16	194	20	−131	4.6
4	77	12	22	5	11	33	53	136	21	123	50	158	4.0
5	78	2	21	8	20	34	1	134	35	153	50	−130	4.0
6	78	4	9	8	43	33	0	136	7	214	40	173	4.3
7	78	5	15	13	35	33	59	134	50	139	60	−138	4.4

Table A2–1 (continued)

NO	DATE Y	M	D	TIME H	M	LAT D	M	LONG D	M	D KM	H KM	AZM D	MAG
8	78	6	20	1	34	33	4	135	2	218	60	−160	4.3
9	78	11	7	15	58	33	41	134	42	173	50	−142	4.4
10	82	5	11	4	19	33	29	135	37	160	30	−172	5.0
11	84	3	20	11	48	32	43.4	135	52.7	243	42	179	5.1
12	85	4	27	2	35	33	52.4	135	24.8	122	40	−161	4.4
REGION 8													
1	77	8	6	2	44	35	11	136	51	96	50	72	4.3
2	81	4	27	5	30	34	51	136	54	97	40	94	4.4
3	81	8	11	13	39	35	4	136	47	87	10	79	4.0
4	81	8	18	23	9	35	17	137	35	164	50	75	5.0
5	81	10	30	9	32	35	12	136	30	68	40	62	3.7
6	83	11	24	10	23	34	43.9	137	42.5	172	36	96	5.0
7	84	8	13	14	37	34	59.9	138	21.6	230	28	87	4.2
REGION 9													
1	76	9	21	15	54	35	47	137	32	181	10	57	4.2
2	78	10	7	5	45	35	47	137	30	179	0	57	5.3
3	78	10	9	0	0	35	46	137	32	180	0	58	4.1
4	79	6	28	21	29	35	48	137	31	181	10	57	4.0
5	84	9	14	9	13	35	47.9	137	29.9	179	7	56	4.5
6	84	9	14	9	36	35	49.7	137	37.1	190	11	57	4.6
7	84	9	14	10	9	35	50.0	137	35.0	188	9	57	4.0
8	84	9	14	12	50	35	48.3	137	29.9	180	8	56	5.0
9	84	9	14	13	41	35	49.7	137	35.1	188	8	57	4.0
10	84	9	15	7	15	35	47.1	137	28.2	177	6	56	6.2
11	84	9	15	7	39	35	47.0	137	29.3	178	9	57	5.6
12	84	9	15	8	16	35	50.2	137	36.1	190	9	57	4.2
13	84	9	15	9	5	35	47.7	137	30.4	180	10	57	5.1
14	84	9	15	16	9	35	50.7	137	34.1	188	8	56	4.1
15	84	9	17	12	22	35	49.3	137	34.5	187	7	57	4.3
16	84	9	24	16	16	35	49.4	137	26.3	177	7	55	4.3
17	84	10	3	9	12	35	49.5	137	37.1	190	5	57	5.3
18	85	4	10	21	56	35	51.1	137	38.5	194	9	57	4.5

* Determined by the Regional Center for Earthquake Prediction, Faculty of Science, Kyoto University.

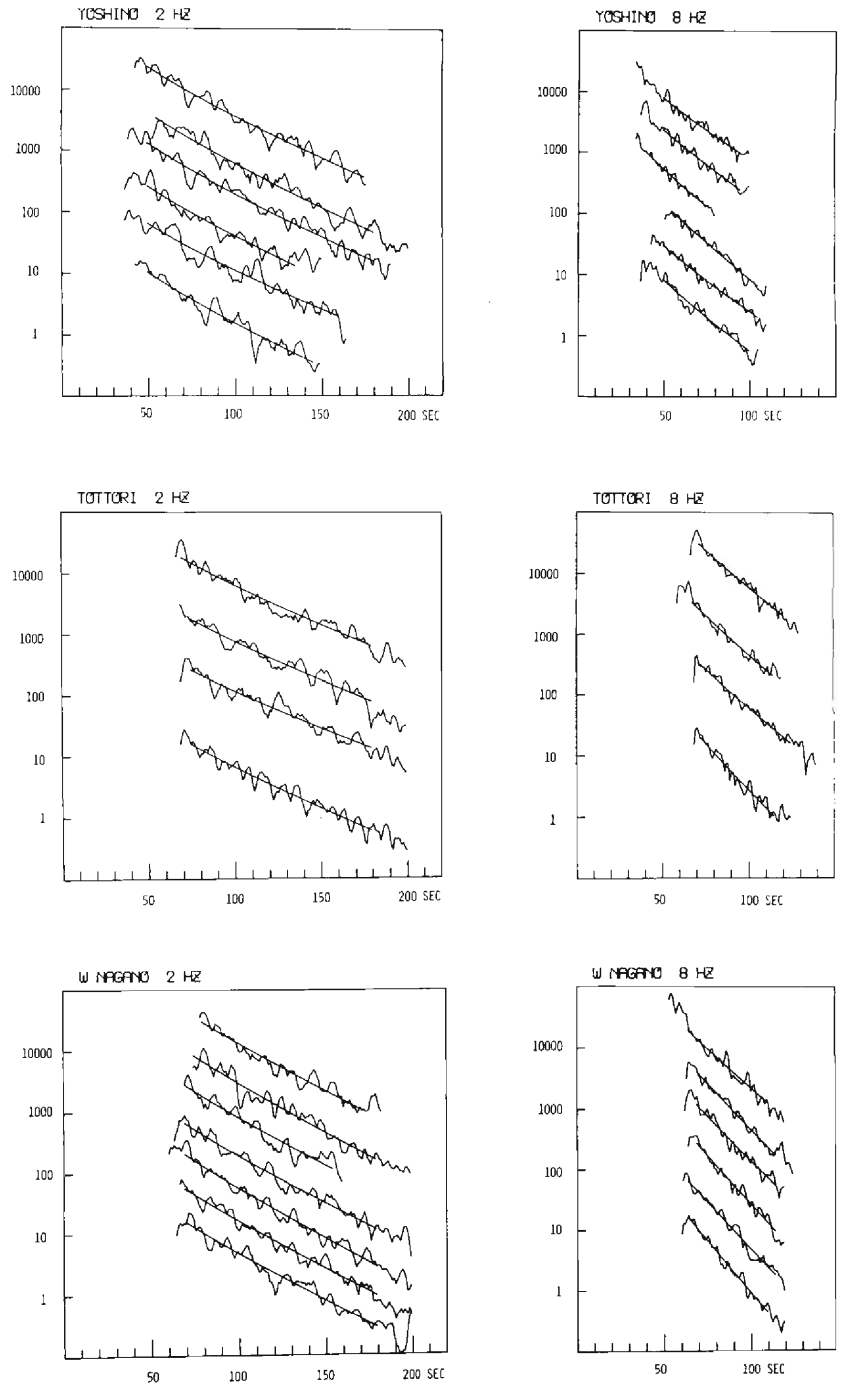

Fig. A2–2 Examples of coda decay. Regional variation of decay may be visible in this raw data.

(1) Close to **SUM**, including the sesimically active region from Lake Biwa to Osaka Bay.
(2) In the northren parts of the Kinki and the adjacent Chubu districts, where the age of the rock formation is considered to be older than that in the southern parts (cf. **Fig. 1**).
(3) The 1983 Tottori earthquake (M 6.2) and its aftershocks.
(4) The earthquakes occurred along the Yamazaki Fault including the aftershocks of the event on May 30 1984 (M 5.6).
(5) Shallow events near Wakayama.
(6) In the source region of the 1952 Yoshino Earthquake (M 7.0) with depth of 60–70 km.
(7) In the Outer Zone, the southren parts to the Median Tectonic Line, with source depth of 20–60 km.
(8) In the central and southern Chubu district.
(9) In the source region of 1984 West Nagano Prefecture Earthquake (M 6.8).

The analyzed intervals of lapse time are 50–180 sec and 80–230 sec according to the hypocentral distance. The interval begins after 30 sec from S arrival in the earliest case. The beginning of the interval is somewhat earlier than that of the coda definition of local earthquake. However, at the time all main parts of L_g waves have passed already, and the coda shows the regular decay as shown by the examples in **Fig. A2–2**, in which the regional variation of the decay can be observed.

The results are listed in **Table A2–2**, and plotted in **Fig. A2–3** in which the regions of (1)–(4) are collected into a group for the Inner Zone, because the meaningful difference may not be visible. As a whole Q_c^{-1} for shallow events is nearly proportional to $f^{-0.5}$, however, the following regional variation may be pointed out:
(a) Q_c^{-1} of (8) and (9) are larger by 20–30% than that of the Inner Zone of the Kinki district, (1)–(4).
(b) Q_c^{-1} of (6), the deepest group, decreases rapidly in the higher frequency range

Table A2–2 Averaged regional Q_c^{-1}
$1000/Q$

REGION	1 Hz	2 Hz	4 Hz	8 Hz	16 Hz	Depth KM
1 R<60 KM	5.01±0.68	3.32±0.62	2.55±0.48	1.78±0.28	1.13±0.13	0–20
2 N KINKI	4.73±0.59	3.20±0.57	2.68±0.56	1.98±0.26	1.13±0.03	0–36
3 TOTTORI	4.91±0.24	3.73±0.21	2.60±0.31	1.80±0.03		11–15
4 YAMAZAKI	4.60±0.73	3.18±0.39	2.38±0.48	1.75±0.24		10–20
5 WAKAYAMA C	4.32±0.81	3.42±0.25	2.62±0.24	1.83±0.27		0– 9
6 YOSHINO	5.01±1.05	3.83±0.42	2.47±0.26	1.48±0.15	0.93±0.09	60–73
7 S KINKI	5.15±1.15	3.76±0.53	2.93±0.25	1.67±0.40		20–60
8 TOKAI	7.47±1.20	4.73±0.76	3.48±0.45	2.37±0.17		10–50
9 W NAGANO	6.84±0.89	4.51±0.58	3.16±0.50	2.33±0.26		0–10

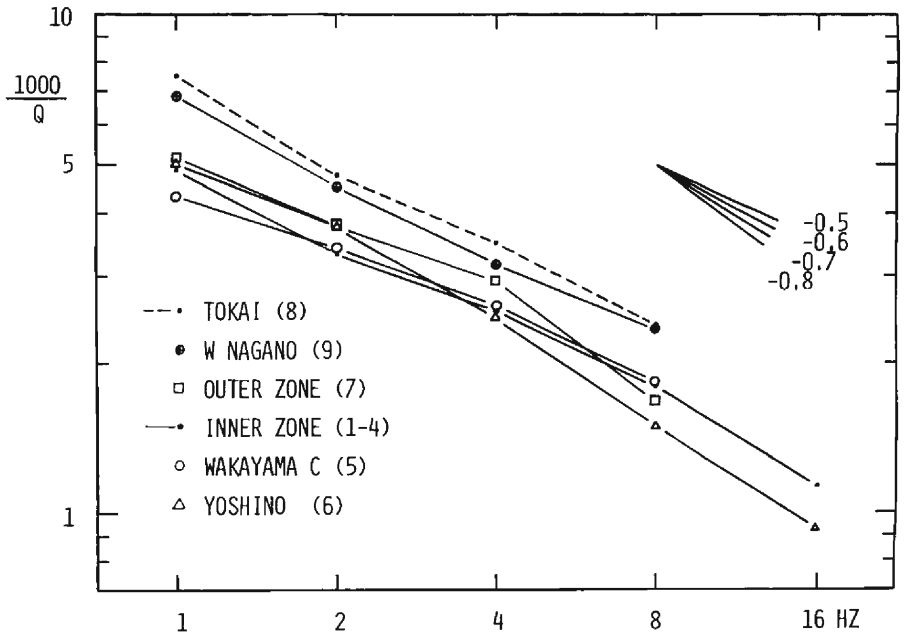

Fig. A2-3 Regional variation of Q_c^{-1}. Q_c^{-1} for the groups of (1)–(4) are averaged and shown as Q_c^{-1} for the Inner Zone.

as $Q_c^{-1} \propto f^{-0.7}$ rather than $f^{-0.5}$.

(c) Q_c^{-1} of (7), the Outer Zone, is slightly larger in the low frequency range of 1–4 Hz than that of the Inner Zone. It decreases rapidly in the higher frequency range. The source depths are rather deep.

(d) Q_c^{-1} of (5), near Wakayama, is nearly the same as that of the Inner Zone, although the region is in the Outer Zone. As the region is near to the **MTL**, Q_c^{-1} may reflect mainly the property of the Inner Zone.